'Tight Binding' methods in quantum transport through molecules and small devices: From the coherent to the decoherent description.

Horacio M. Pastawski[1] and Ernesto Medina[2]

[1] *Facultad de Matemática, Astronomía y Física, Universidad Nacional de Córdoba, Ciudad Univeritaria, 5000 Córdoba, Argentina*

[2] *Laboratorio de Física Estadística de Sistemas Desordenados, Centro de Física, Instituto Venezolano de Investigaciones Científicas, Caracas, Venezuela*

We discuss the steady-state electronic transport in solid-state and molecular devices in the quantum regime. The decimation technique allows a comprehensive description of the electronic structure. Such a method is used, in conjunction with the generalizations of Landauer's tunneling formalism, to describe a wide range of transport regimes. We analize mesoscopic and semiclassical metallic transport, the metal-insulator transition, and the resonant tunneling regime. The effects of decoherence on transport is discussed in terms of the D'Amato-Pastawski model. A brief presentation of the time dependent phenomena is also included.

Keywords: Quantum coherence; Green's functions; resonant tunneling

Se discute el transporte, en el estado estacionario, en dispositivos moleculares y de estado sólido en el régimen cuántico. La técnica de decimación permite una descripción completa de la estructura electrónica. Tal método, en conjunto con la generalización del formalismo de Landauer, puede ser usado para describir un rango amplio de regímenes de transporte. Se analiza el transporte mesoscópico y semiclásico en el régimen metálico, la transición metal-aislante, y el régimen de túnel resonante. Los efectos de decoherencia en el transporte son tratados en términos del modelo de D'Amato-Pastawski. Finalmente se incluye una breve presentación de fenómenos dependientes del tiempo.

Descriptores: Coherencia cuántica; funciones de Green; tunelamiento resonante

PACS: 31.15.-p; 73.21.-b; 73.63.-b

I. INTRODUCTION

With the advent of progressive miniaturization of electronic devices, it becomes necessary to describe the transport properties of small systems within a fully quantum mechanical framework. As a representative example, we just recall the double barrier resonant tunneling device[1] (DBRTD), whose current-voltage ($\mathsf{I}-\mathsf{V}$) curve presents a well defined peak as shown in Fig.1 adapted from data in reference[2]. This behavior, in great departure from the usual monotonic features shown by macroscopic samples, can be attributed to quantum interference phenomena, which arises from the coherent dynamics of the carriers.

Let us characterize a "device", in a rough sense, as some specified region of material where the carriers spend a substantial part of the time. It might be characterized by a longitudinal length L_x and a transverse cross section $L_y \times L_z = M\, a^2$, where a is an atomic length scale. In order to manifest its wave nature, an electronic excitation must propagate quantum mechanically (i.e. phase coherently) between these boundaries. Typical interference phenomena occurs when any of these lengths is comparable with the deBroglie wavelength λ_ε. A condition for this quantum coherence is the weak coupling with the environmental degrees of freedom within the relevant time scales. This condition can often be achieved by shrinking the device length scales and/or lowering the temperatures until the minimum energy excitation Δ becomes large compared to the available thermal energy $k_B T$. In the experiment of Fig.1 the applied voltage is the control parameter for the wave length of the electrons responsible for the transport. Therefore, the peaked $\mathsf{I}-\mathsf{V}$ curve of the DBRTD can be viewed much as resonant peaks in a Fabry-Perrot interferometer.

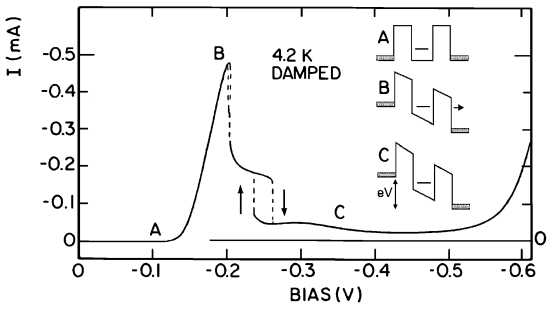

FIG. 1. Scheme of a DBRTD and experimental current-voltage characteristic. Results adapted from Ref. 2. The points A, B and C in the curve corresponds to the potential profile shown in the inset.

A great variety of solid-state devices developed in

the last decade[3] satisfy the general conditions for the quantum manifestations described above. More recently, the growing interest[4] in understanding the conductance between two electrodes connected through a bridging molecule lies naturally in this category. In fact, discreteness of the molecular electronic energy levels is a clear manifestation of the quantum coherence of the electronic states and one is left with the question of how do these states transport charge[5]. The related issue of the propagation of a charge density excitation has been tackled by physical-chemists who, for a long time, have been dealing with problems as diverse as conducting polymers[6], charge oscillation in the intermediate valence compounds[7] (e.g. the Creutz-Taube ion $(NH_3)_5$Ru-pyz-Ru-$(NH_3)_5$ $^{+5}$ where pyz stands for pyrazine) and electron transfer in photosynthetic systems[8].

The traditional methods used to describe transport are not necessarily appropriate for mesoscopic and molecular systems. The semiclassical Boltzmann equation, the Kubo formalism and other traditional techniques were specially devised to describe bulk transport, where the thermodynamic limit is guaranteed and the linear response regime is the relevant one. Hence, in order to deal with transport in finite size "samples" with non trivial geometrical constrains, and often in presence of non-perturbative fields, a new perspective had to be adopted. It is clear that a general Schrödinger equation must provide the complete description. However, even in the simplest independent particle approximation, it seems difficult to include the complex boundary conditions imposed by the electrodes. A way out is to treat transport of carriers through the "sample " as a scattering problem from one electrode to the other. Therefore, the transmittance T undertakes a most relevant role. This is essentially the conceptual framework on which the Landauer's description[9] of transport is based. It involves a simple but conceptually new approach that inspired most of the advances in solid-state devices in recent years and is now clearing the way towards molecular electronics.

In this article, we attempt to present a self-contained operational and conceptual manual based on the lectures given by the authors at the 2nd Workshop on Mesoscopic Systems. We will attempt to summarize the methods used to evaluate and interpret the electronic structure of finite systems, as well as how they are extended to describe the coherent transport when they are connected to electrodes. While the effects of electron-electron interaction can become of utmost relevance in small systems[10,11], for didactic reasons we will not extend on this blooming field. Let's only mention that their understanding[12] is built upon the methods and ideas we describe in this review.

The material is presented as follows: Section II is devoted to Landauer's ideas, and represents the backbone over which the formalism is built. Section III introduces the decimation method to calculate transmittances and electronic structure of devices and molecules. Section IV shows the connection between electronic-structure and transport obtained by Fisher and Lee. Their formula is derived and discussed there. Section V presents an overview of the known results of transport which can help the beginner to see the machinery in action. Section VI is devoted to the introduction of decoherence into the formalism. Section VII presents a brief outline of the time-dependent problem.

A number of the most simple calculations will be worked out with some detail, so the unfamiliar reader might acquire a first feel for the topic by noting the simplicity of the methodology. The most advanced results will be left merely indicated so that they can be reobtained by a motivated reader. Many of the examples presented here are completely original and have not been published before to our knowledge. Finally, let us stress that we do not attempt to review the literature exhaustively, but simply to present our personal pathway through the concepts involved. In particular, the issues of decoherence and time dependence are the object of current research and the reader might still create his own trek.

II. THE BASIC IDEAS OF LANDAUER

Rolf Landauer was the first to realize that, besides the "sample " or device one must explicitly incorporate the electrodes or contacts in the transport description. He introduced two one-dimensional wires, left (L) and right (R), connecting "the sample" to electron reservoirs. The net current leaving the lead L is expressed in terms of the number of electrons available in the leads, their typical velocity and the probability $T_{R,L}$ of transmission through the sample

$$\mathsf{I}_L = e \int [T_{R,L}(\varepsilon) v_L \frac{1}{2} N_L(\varepsilon) f_L(\varepsilon) - T_{L,R}(\varepsilon) v_R \frac{1}{2} N_R(\varepsilon) f_R(\varepsilon)] \mathrm{d}\varepsilon. \quad (1)$$

The meaning of this equation is obvious: it balances currents. Each reservoir i emits electrons with an energy availability controlled by a local distribution function $f_i(\varepsilon) = 1/[\exp[(\varepsilon - \mu_i)/k_B T + 1]$, where ε is the energy and $\mu_i = \mu_o + \delta\mu_i$ is the chemical potential which is displaced from its equilibrium value μ_o. The density of those "outgoing" states is $\frac{1}{2}N_i(\varepsilon)$ (half the total) and their velocity v_i. The coefficient $T_{R,L}$ computes current as positive provided that the particle can pass through the sample. Taking the $i = L$ reservoir as reference, the first term is then an "out " current while the second is the "in" contribution. It was essential in Landauer's reasoning to note that in a propagating channel the density of states N_i is inversely proportional to the corresponding group velocity:

$$N_i \equiv \frac{2}{v_i h}. \quad (2)$$

This fundamental fact remained unnoticed in the previous discussions of quantum tunneling[1] and it is the key to understand conductance quantization. Notice that there is no use for the traditional $[1 - f_j(\varepsilon)]$ factor to exclude transitions to occupied final states. In a scattering formulation, the final "out" states are already contained in the "in" states[13]. Although different "in" states (e.g. on the left and right leads) could end in the same final state, unitarity of quantum mechanics assures that outgoing contributions are orthogonal.

To obtain the usual Landauer *two probe* conductance, one assumes time reversal for the transmittances: $T_{R,L} = T_{L,R}$. At low temperatures, the Fermi distribution function can be safely replaced by a step function. If *linear response* can be invoked ($\delta\mu_i = \mu_i - \varepsilon_F \ll \varepsilon_F$), the integral is approximated by using the transmittance evaluated at a Fermi energy. If we do not include the usual factor of 2 due to the spin degeneracy, one gets

$$\mathsf{I} = \frac{e}{h} T_{R,L}(\delta\mu_L - \delta\mu_R) \text{ where } (\delta\mu_L - \delta\mu_R) = e\mathsf{V} \quad (3)$$

from which the two-probe conductance can be calculated

$$\mathsf{G}_{R,L} = \frac{e^2}{h} T_{R,L}. \quad (4)$$

This conductance accounts for the "sample-lead" system. In a perfect 1-d conductor $T_{R,L} = 1$, and it remains finite. In fact, resistance results $h/e^2 = 25.812K\Omega$ per channel, the quantum value found later in the Quantum Hall Effect. In contrast, the original Landauer's conductance

$$\mathsf{G}^{\text{f.p.}}_{R,L} = \frac{e^2}{h} \frac{T_{R,L}}{1 - T_{R,L}} \quad (5)$$

is an attempt to extract an intrinsic property of the "sample". This conductance corresponds to a *four probe measurement,* as shown in Fig. 2 (upper panel) where two leads are used to inject and drain the current respectively, while the other two additional "non-invasive" probes, denoted by A and B, are used to measure the voltage drop in the "sample" neighborhood. They are very weakly coupled wires or capacitive "non-invasive" probes. The difference,

$$\mathsf{R}^{\text{contact}} = 1/\mathsf{G}_{R,L} - 1/\mathsf{G}^{\text{f.p.}}_{R,L} = \frac{h}{e^2}, \quad (6)$$

can be interpreted as a contact resistance associated to the lead-sample interface.

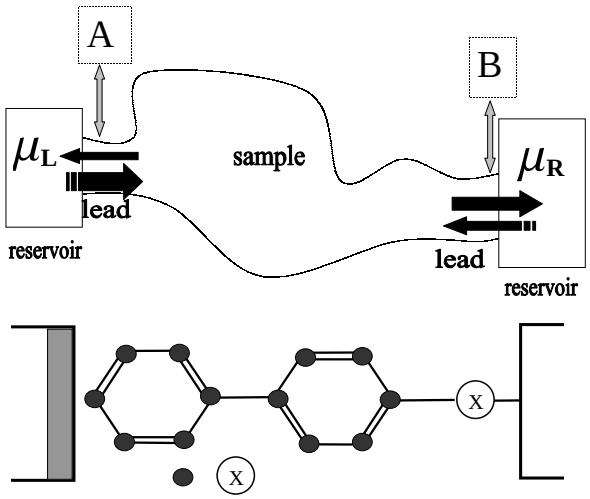

FIG. 2. Upper panel: Landauer's representation of a general electronic transport experiment. Lead at left (L) and right (R) inject and extract current. Weakly coupled voltage probes A and B at the "sample" boundaries are also represented. Lower Panel: Portion of an actual molecular sandwich heterostructure between a Au-Ti left electrode and a right Au electrode. The bridge molecule is 4-4-thioacetilbiphenyl. The residue at right (X =S, Se, Te) can be substituted.

A more general formulation of Eqs.(1) and (2) for a system composed by many channels (e.g. spin and transversal modes) subject to different boundary conditions results from the application[14] of the Kirchoff law using Landauer's conductances

$$\mathsf{I}_i = \frac{e}{h} \sum_j \int [T_{j,i}(\varepsilon) f_i(\varepsilon) - T_{i,j}(\varepsilon) f_j(\varepsilon)] \mathrm{d}\varepsilon. \quad (7)$$

We do not exclude sites $i = j$ from the sum. Here, the transmission coefficients may depend on the external parameters such as voltages, and hence accounts for non-linear response. The non-ohmic $\mathsf{I} - \mathsf{V}$ curve of the DBRTD shown in Fig.1 can indeed be obtained directly from this formula by summing up over transversal quantum numbers (channels) in the left and right leads. Also $\mu_i = \mu_L$ for every outgoing channel in the left lead and $\mu_i = \mu_R$ for every outgoing channel in the right lead.

Having understood the basic requirements of a transport theory one must learn to connect the transmittances T with the electronic properties of the "sample" and electrodes. In the treatment of solid state devices many researchers adopted the strategy of modeling the transport through the scattering matrices. However, when one deals with a molecular system, it becomes clear that specific features of the electronic structure at the molecular level are relevant. Thus, at least an approximate description of these properties through Hamiltonian models is mandatory. Let us remark that in the Landauer formalism, the "sample" is considered a finite system while the electrodes are considered in their thermodynamic limit

with a continuum spectrum and acting as charge reservoirs. One then needs a formulation capable of dealing naturally with both situations.

III. ELECTRONIC PROPERTIES THROUGH REAL SPACE RENORMALIZATION GROUP PROCEDURES.

A. Origin of the tight-binding model

The first thing we want to point out is that tight binding models, although naturally associated with *linear combination of atomic orbitals* (LCAO) can also be obtained as a convenient approximation to the Schrödinger equation written in terms of the continuous coordinate x

$$-\frac{\hbar^2}{2m}\nabla^2\psi(x)+U(x)\psi(x)=\varepsilon\psi(x) \tag{8}$$

We can discretize this equation obtaining a finite differences approach

$$-\frac{\hbar^2}{2m}\frac{\dfrac{\psi(x+\Delta x)-\psi(x)}{\Delta x}-\dfrac{\psi(x)-\psi(x-\Delta x)}{\Delta x}}{\Delta x}+U(x)\psi(x)=\varepsilon\psi(x) \tag{9}$$

If we do the identifications

$$\begin{array}{ll}\Delta x=a; & x=na; \quad u_n=\psi(na);\\ E_n=U(x_n); & V=\frac{\hbar^2}{2ma^2};\end{array} \tag{10}$$

we finally obtain:

$$(\varepsilon-E_n)u_n-Vu_{n+1}-Vu_{n-1}=0. \tag{11}$$

Therefore, one is left with a discrete equation where the interaction is provided by the *kinetic energy* terms V which is usually short ranged. The *local potential energy* term is given by E_n and, in the LCAO description, it can be identified with the energies of atomic orbitals.

The above relation can be used in a "reversible" way since there are situations where calculations in the continuum are simpler, as occurs in the semiclassical limit when the WKB approsimation substantially simplify the problem.

Indeed, when the discretization is done at a scale much smaller than the typical atomic scale $\Delta x \ll a_0$ one can reach the molecular scale of the LCAO by a progressive use of the procedure that is discussed in the following paragraph. For the moment, we consider the tight binding Hamiltonian:

$$\hat{\mathcal{H}}=\sum_n E_n\left|n\right\rangle\left\langle n\right|+V_{n,n+1}\left|n\right\rangle\left\langle n+1\right|+V_{n+1,n}\left|n+1\right\rangle\left\langle n\right|, \tag{12}$$

with $\langle n\left|\psi\right\rangle=u_n$, $E_n\equiv E_o$ and $V_{n,n+1}=-V$, from which the Schrödinger Eq.(12) takes the matrix form

$$\varepsilon\begin{pmatrix}\vdots\\ u_{n-1}\\ u_n\\ u_{n+1}\\ \vdots\end{pmatrix}-\begin{pmatrix}\ddots & & & & \\ & E_{n-1} & V_{n-1,n} & 0 & \\ & V_{n,n-1} & E_n & V_{n,n+1} & \\ & 0 & V_{n+1,n} & E_{n+1} & \ddots\\ & & & & \ddots\end{pmatrix}\begin{pmatrix}\vdots\\ u_{n-1}\\ u_n\\ u_{n+1}\\ \vdots\end{pmatrix}=(\varepsilon\mathbf{I}-\mathbf{H})\,\overrightarrow{u}=\overrightarrow{0}. \tag{13}$$

When the site energies are taken from a random distribution in the range $[-W/2,W/2]$ the Hamiltonian is referred to as the Anderson model and it is the standard model to represent disordered systems.

In a general situation of a LCAO problem, E_n corresponds to any of the specific atomic orbitals used for each atom and the interactions parameters might not be restricted to first neighbors complicating the topology of the interaction network.

B. Effective Hamiltonians and Green's functions

Let's see how to construct a progressive solution of this problem[15] using the ideas of the real space renormalization group[16,17].

The simplest case is the two site problem

$$\varepsilon \begin{pmatrix} u_1 \\ u_2 \end{pmatrix} - \begin{pmatrix} E_1 & V_{1,2} \\ V_{2,1} & E_2 \end{pmatrix} \begin{pmatrix} u_1 \\ u_2 \end{pmatrix} = 0, \tag{14}$$

whose energy spectrum is obtained from the secular equation

$$\det |\varepsilon \mathbf{I} - \mathbf{H}| = 0, \tag{15}$$

with eigenvalues

$$E_{\pm} = \left(\frac{E_1 + E_2}{2} \right) \pm \sqrt{\left(\frac{E_1 - E_2}{2} \right)^2 - V_{1,2} V_{2,1}}. \tag{16}$$

An alternative procedure is to write the linear equation explicitly

$$\begin{array}{ll} a) & E_1 u_1 + V_{1,2} u_2 = \varepsilon u_1, \\ b) & V_{2,1} u_1 + E_2 u_2 = \varepsilon u_2. \end{array} \tag{17}$$

From $b)$ $u_2 = V_{2,1} \frac{1}{\varepsilon - E_2} u_1$, and substituting in $a)$:

$$\left(E_1 + V_{1,2} \frac{1}{\varepsilon - E_2} V_{2,1} \right) u_1 = \varepsilon u_1. \tag{18}$$

The eigenvalue is obtained from the condition

$$\varepsilon - [E_1 + \underbrace{V_{1,2} \frac{1}{\varepsilon - E_2} V_{2,1}}_{\Delta_1(\varepsilon)}] = 0 \tag{19}$$

The reader can check that *both exact eigenenergies*, can be obtained from this equation. The second term in the parenthesis has a clear physical meaning if it is identified with an "effective potential" $\Delta_1(\varepsilon) = \frac{|V_{1,2}|^2}{\varepsilon - E_2}$ which corrects the non-interacting energy E_1 of the site as

$$\widetilde{E}_1 = E_1 + \Delta_1(\varepsilon). \tag{20}$$

For an asymmetric case, $|E_1 - E_2| > |V_{1,2}|$, one can obtain a good approximation to the corrected site energies, by doing the evaluation at the old eigenvalue:

$$\widetilde{E}_1 \simeq E_1 + \Delta_1(E_1), \tag{21}$$

which becomes equivalent to the second order Rayleigh-Schrödinger perturbation theory. That is, as shown in Fig.3, we have gone from the two orbital problem to a single effective orbital with a "dressed energy ".

C. The Decimation Method

The preceding paragraphs have introduced the basic tools by noting that the presence of other sites has the effect of shifting or splitting the energies of the site we are looking at. Let us see another example, a Hamiltonian with three sites:

$$\begin{pmatrix} E_1 & V_{1,2} & V_{1,3} \\ V_{2,1} & E_2 & V_{2,3} \\ V_{3,1} & V_{3,2} & E_3 \end{pmatrix} \begin{pmatrix} u_1 \\ u_2 \\ u_3 \end{pmatrix} = \varepsilon \begin{pmatrix} u_1 \\ u_2 \\ u_3, \end{pmatrix} \tag{22}$$

where we have included second neighbor overlaps. The idea is to reduce this set of three linear equations to a smaller problem as shown in Fig.4. There are many situations where the physics and chemistry indicates that this is a physically meaningful model. We obtain the value of u_2 from the second row above

$$u_2 = \frac{V_{2,1}}{\varepsilon - E_2} u_1 + \frac{V_{2,3}}{\varepsilon - E_2} u_3, \tag{23}$$

and introduce it into the first and third row to obtain two coupled non-linear equations:

$$\begin{pmatrix} \widetilde{E}_1 & \widetilde{V}_{1,3} \\ \widetilde{V}_{3,1} & \widetilde{E}_3 \end{pmatrix} \begin{pmatrix} u_1 \\ u_3 \end{pmatrix} = \varepsilon \begin{pmatrix} u_1 \\ u_3 \end{pmatrix}, \tag{24}$$

where

$$\begin{aligned} \widetilde{E}_1(\varepsilon) &= E_1 + V_{1,2} \frac{1}{\varepsilon - E_2} V_{2,1}, \\ \widetilde{E}_3(\varepsilon) &= E_3 + V_{3,2} \frac{1}{\varepsilon - E_2} V_{2,3}, \\ \widetilde{V}_{1,3} &= V_{1,3} + V_{1,2} \frac{1}{\varepsilon - E_2} V_{2,3}, \end{aligned} \tag{25}$$

and the notation is self-explanatory.

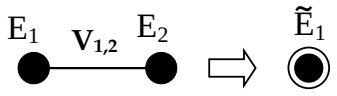

FIG. 3. Construction of the self-energy correction.

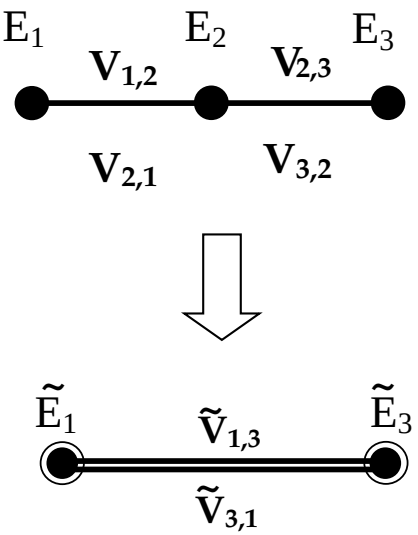

FIG. 4. Construction of an effective Hamiltonian through decimation.

Therefore, the procedure of elimination of variables is very general and can exhaust the degrees of freedom of the finite system, providing a systematic way to reduce the dimension of the Hamiltonian. This is done at the cost of transforming the linear equation into a non-linear one which, however, can often be linearized in the region of interest as in Eq. (21). The general recipe valid for a string of interacting atoms requires the calculation of:

- $\Delta^{+}_{1(n)}$, the energy correction to the $1^{\rm st}$ atom when sites until atom n, to the right (+) inclusive, are eliminated.
- $\Delta^{-}_{n+1}(\varepsilon)$, the energy correction to atom $(n+1)$ when all the atoms at the left (-), except the $1^{\rm st}$, have been eliminated.
- $\widetilde{V}_{1,n+1}$, the effective interaction among layers.

We resort to the recursion formulas:

$$\Delta^{+}_{1(n)}(\varepsilon) = \Delta^{+}_{1(n-1)} + \widetilde{V}_{1,n}\frac{1}{\varepsilon - E_n - \Delta^{-}_{n}}\widetilde{V}_{n,1} \tag{26}$$

$$\Delta^{-}_{n+1}(\varepsilon) = V_{n+1,n}\frac{1}{\varepsilon - E_n - \Delta^{-}_{n}}V_{n,n+1} \tag{27}$$

$$\widetilde{V}_{1,n+1} = \widetilde{V}_{1,n}\frac{1}{\varepsilon - E_n - \Delta^{-}_{n}}V_{n,n+1} + V_{1,n+1} \tag{28}$$

Notice that we have not restricted the iterations to nearest neighbors. From the point of view of the perturbation theory, it can be checked that the decimation procedure is equivalent to an exact summation of all the perturbation orders of the Wigner-Brillouin series and hence equivalent to the inclusion of all Feynman paths that start at layer 0 and end at layer $N+1$. This will be best viewed in the language of the Green's function described in the next subsection.

D. Effective Hamiltonians and Green's functions

The Green's function provides an alternative framework to discuss the solutions of the Schrödinger equation. Besides the intuitive structure of the perturbative calculations in terms of Feynman diagrams[18], they have the additional advantage of a clear connection to transport properties, and finally a special role in the Quantum Field Theory which allows a definitive treatment of the many-body problems.

The retarded (advanced) Green's functions matrix is defined as a function of the complex variable $(\varepsilon \pm \mathrm{i}\eta)$ in the upper (lower) complex plane.

$$\mathbf{G}^{R(A)}(\varepsilon) = [(\varepsilon \pm \mathrm{i}\eta)\mathbf{I} - \mathbf{H}]^{-\mathbf{1}}. \tag{29}$$

Let's evaluate a diagonal element:

$$\begin{aligned} G^{R}_{1,1}(\varepsilon + \mathrm{i}\eta) &= \frac{1}{\varepsilon + \mathrm{i}\eta - E_1 - \underbrace{V_{1,2}\frac{1}{\varepsilon + \mathrm{i}\eta - E_2}V_{1,2}}_{\Sigma^{R}_{1} = \Delta_1 - \mathrm{i}\Gamma_1}} \\ &= \frac{1}{\varepsilon + \mathrm{i}\eta - \widetilde{E}_1}. \end{aligned} \tag{30}$$

Therefore the renormalized site energy is as before

$$\widetilde{E}_1 = E_1 + \underbrace{V_{1,2}\frac{1}{\varepsilon + \mathrm{i}\eta - E_2}V_{2,1}}_{\Sigma^{R}_{1} = \Delta_1 - \mathrm{i}\Gamma_1} \tag{31}$$

The local densities of states represents the weight of the exact eigenenergies on the old states, which we can check for our simple two state model, is:

$$N_1(\varepsilon) = |u_{1,+}|^2\,\delta(\varepsilon - E_+) + |u_{1,-}|^2\,\delta(\varepsilon - E_-) \tag{32}$$

$$= \lim_{\eta\to 0}\left\{|u_{1,+}|^2\,\frac{1}{\pi}\frac{\eta}{(\varepsilon - E_+)^2 + \eta^2} + |u_{1,-}|^2\,\frac{1}{\pi}\frac{\eta}{(\varepsilon - E_-)^2 + \eta^2}\right\}, \tag{33}$$

where $\delta(\varepsilon - E_\pm)$ are the Dirac delta functions at $E_\pm = \frac{1}{2}[(E_1 + E_2) \pm \hbar\omega]$, with $\hbar\omega = \sqrt{(E_1 - E_2)^2 + 4\,|V_{1,2}|^2}$. The eigenstates are $|+\rangle = u_{1,+}\,|1\rangle + u_{2,+}\,|2\rangle$ and $|-\rangle = u_{1,-}\,|1\rangle + u_{2,-}\,|2\rangle$ with the coefficients

$$u_{1,\pm} = \left\{\frac{V_{1,2}}{2\,|V_{1,2}|^2}\left[1 \pm \frac{E_1 - E_2}{\hbar\omega}\right]\right\}^{1/2}, \tag{34}$$

$$u_{2,\pm} = \pm\left\{\frac{V_{1,2}}{2\,|V_{1,2}|^2}\left[1 \mp \frac{E_1 - E_2}{\hbar\omega}\right]\right\}^{1/2}. \tag{35}$$

An immediate advantage of the Green's function formalism is that although it is obtained through a finite number of algebraic operations (matrix inversion) it contains information on both the eigenenergies and eigenfunctions which involve the transcendental operation of finding the roots of a polynomial. In particular, any eigenvector component is obtained from the generalization of Eq. (32) which results:

$$N_i(\varepsilon) = -\frac{1}{\pi}\lim_{\eta\to 0}\mathrm{Im}G^R_{i,i}(\varepsilon+\mathrm{i}\eta) \tag{36}$$

The connection with the infinite order perturbation theory is immediate just expressing the denominator in Eq. (30) through its series expansion

$$G^R_{1,1}(\varepsilon) = \frac{1}{\varepsilon+\mathrm{i}\eta - E_1 - V_{1,2}\dfrac{1}{\varepsilon+\mathrm{i}\eta-E_2}V_{1,2}}, \tag{37}$$

$$= \frac{1}{\left[G^{(o)R}_{1,1}(\varepsilon)\right]^{-1} - V_{1,2}G^{(o)R}_{2,2}(\varepsilon)V_{2,1}} \tag{38}$$

$$= G^{(o)R}_{1,1}(\varepsilon)[1-\sum_{n=0}^{\infty}\left(V_{1,2}G^{(o)R}_{2,2}(\varepsilon)V_{2,1}\right)^n] \tag{39}$$

$$= G^{(o)R}_{1,1}(\varepsilon) + G^{(o)R}_{1,1}(\varepsilon)V_{1,2}G^{(o)R}_{2,2}(\varepsilon)V_{2,1}G^{(o)R}_{1,1}(\varepsilon) + \cdots, \tag{40}$$

$$= G^{(o)R}_{1,1}(\varepsilon) + G^{(o)R}_{1,1}(\varepsilon)\Sigma_{1,1}(\varepsilon)G^R_{1,1}(\varepsilon) \tag{41}$$

The last line corresponds to the Dyson equation while the series expansion is represented diagrammatically in Fig.5.

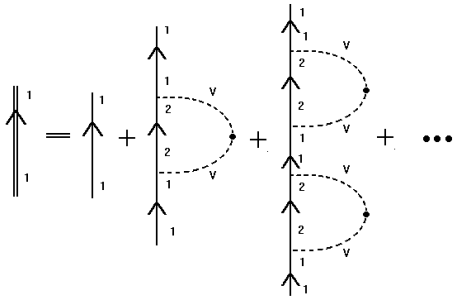

FIG. 5. Feynman diagrams in tight-binding representation. Double and simple lines represent the exact and unperturbed Green's function respectively. Hopping interactions are represented by the dashed lines that modifies the indices of a Green's function. Two conjugate interactions are associated by the dot into a single rung.

In systems with a finite number, N, of states $G_{i,j}(\varepsilon)$ is a well behaved meromorphic function except at the N poles. In this condition, it is satisfied that

$$\text{finite system}\begin{cases}\Gamma(\varepsilon) = -\mathrm{Im}[\Sigma(\varepsilon)] \equiv 0,\\ \Sigma(\varepsilon)\equiv\Delta(\varepsilon) = \mathrm{Re}[\Sigma(\varepsilon)].\end{cases} \tag{42}$$

Therefore, by considering real energies we can drop the supra-index that distinguish the retarded and advanced Greens function.

Let us come back to the three site model. We may sum up the infinite perturbation series to obtain

$$G_{1,1}(\varepsilon) = \frac{1}{\varepsilon - E_1 - V_{1,2}\dfrac{1}{\varepsilon - E_2 + V_{2,3}\dfrac{1}{\varepsilon-E_3}V_{3,2}}V_{2,1} - V_{1,3}\dfrac{1}{\varepsilon-E_3}V_{3,1}}, \tag{43}$$

or equivalently use Eq. (25) to regrouping the terms into:

$$G_{1,1}(\varepsilon) = \frac{1}{\varepsilon - \widetilde{E}_1 - \widetilde{V}_{1,3}\dfrac{1}{\varepsilon-\widetilde{E}_3}\widetilde{V}_{3,1}}, \tag{44}$$

which gives the obvious connection with the real space decimation procedure.

Many other useful recursion formulas can be obtained by similar procedures. For example, in a system with states $\{0,1,2,3,\cdots N,N+1\}$, the effective hopping is related to the non-diagonal Green's function in the isolated bridge with states $\{1,2,3,\cdots N\}$,

$$\widetilde{V}_{0,N+1} = \widetilde{V}_{0,N}\left[\varepsilon - \widetilde{E}_N\right]^{-1}V_{N,N+1}, \tag{45}$$

$$= V_{0,1}\left\{G_{1,N-1}V_{N-1,N}\left[\varepsilon - E_N - \Delta^-_N\right]^{-1}\right\}V_{N,N+1},$$
$$= V_{0,1}\left\{G_{1,N}\right\}V_{N,N+1}. \tag{46}$$

This equation is complemented with the ones for the self-energies from sites at right

$$\Delta^+_{0(N)}(\varepsilon) = V_{0,1}G_{1,1}V_{1,0}, \tag{47}$$

and at left

$$\Delta^-_{N+1(N)}(\varepsilon) = V_{N,N+1}G_{N,N}V_{N,N+1}. \tag{48}$$

One can then calculate by iteration of the non-diagonal Greens Function in progressively bigger systems

$\{0, \cdots N+2\}$, $\{0, \cdots N+3\}$, and so on, with an equation that is obtained equating the terms between brackets in Eq.(45):

$$G^{(N+1)}_{1,N+1} = G^{(N)}_{1,N} V_{N,N+1} G^{(N+1)}_{N+1,N+1}, \tag{49}$$

which is used in conjunction with,

$$G^{(N+1)}_{N+1,N+1} = \left[\varepsilon I - E_{N+1} - V_{N+1,N} G^{(N)}_{N,N} V_{N+1,N}\right]^{-1}, \tag{50}$$

the continued fraction expansion of the diagonal Greens function.

E. Going beyond one-dimensional systems.

The decimation scheme can be generalized to any dimension as long as we proceed in a "layer by layer" elimination. Every site in the above procedure now becomes an $n \times n$-matrix where n is the size of the layer. In Fig. 6 we consider a square lattice of orbitals forming a strip. Remembering that $\mathrm{Im}[\mathbf{\Sigma}] \equiv 0$ we write the general equation for the real self-energies. We proceed to eliminate one by one the layers from 1 to the $(N-1)$. Adopting the matrix notation $\mathbf{\Delta}^{+}_{1(n)}(\varepsilon)$ is the self-energy correction to the 1^{st} layer when all layers (to the right) including the n^{th} have been eliminated. $\mathbf{\Delta}^{-}_{n+1}(\varepsilon)$ is the self-energy correction to layer $(n+1)$ when layers to the left have been eliminated. $\widetilde{\mathbf{V}}_{1,n+1}$ is the effective interaction between layers. These are again evaluated with the iterative procedure

$$\mathbf{\Delta}^{+}_{1(n)}(\varepsilon) = \mathbf{\Delta}^{+}_{1(n-1)} + \widetilde{\mathbf{V}}_{1,n} \frac{1}{\varepsilon \mathbf{I} - \mathbf{E}_n - \mathbf{\Delta}^{-}_{n}} \widetilde{\mathbf{V}}_{n,1}, \tag{51}$$

$$\mathbf{\Delta}^{-}_{n+1}(\varepsilon) = \mathbf{V}_{n+1,n} \frac{1}{\varepsilon \mathbf{I} - \mathbf{E}_n - \mathbf{\Delta}^{-}_{n}} \mathbf{V}_{n,n+1}, \tag{52}$$

$$\widetilde{\mathbf{V}}_{1,n+1} = \widetilde{\mathbf{V}}_{1,n} \frac{1}{\varepsilon \mathbf{I} - \mathbf{E}_n - \mathbf{\Delta}^{-}_{n}} \mathbf{V}_{n,n+1} + \mathbf{V}_{1,n+1}, \tag{53}$$

with the initial values:

$$\begin{array}{c} \mathbf{\Delta}^{+(1)}_{1}(\varepsilon) = 0, \\ \mathbf{\Delta}^{-}_{2}(\varepsilon) = 0, \\ \widetilde{\mathbf{V}}_{1,2} = \mathbf{V}_{1,2}. \end{array} \tag{54}$$

The expression one has to evaluate are expressed as Matrix Continued Fractions, which are numerically very stable[19]. Notice that the elimination of intermediate layers produces effective interaction among the sites in the first layer, i.e. it modifies the intra-layer interactions as prescribed by the non-diagonal elements of $\mathbf{\Delta}$. Interlayer interactions are always contained in $\mathbf{V}$. Again, the last term in Eq. (53) allows the consideration of interactions going beyond nearest neighbor layers.

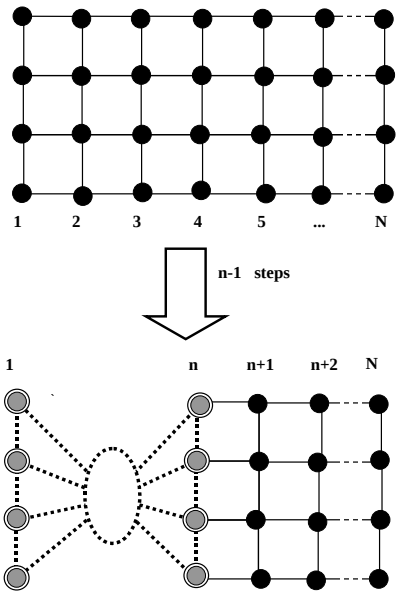

FIG. 6. Scheme of the decimation of a finite tight-binding strip. As the elimination of intermediate layers proceeds the effective site energies and interaction appears.

F. Decimation in Molecules

It is clear that the described procedure is very well suited for application to molecular systems[15,20]. Just to fix ideas consider the p_z orbitals in the carbon backbone of an organic molecule represented in Fig.7. Assume that we are interested in the study of how charge can be transferred from site L to site R, a typical problem in photosynthesis and molecular electronics. Circles represent the π orbitals with given local energies, lines are hopping interactions which produce the electron delocalization. One might start decimating the dangling ends. Sites energies in the back-bone are then renormalized. Next, we identify the branching nodes and eliminate the bridging sites, this gives new site energies and an effective hopping. Finally one eliminates all the remaining bridging structure obtaining an effective two orbital molecule. Since the procedure is exact one obtains the exact spectrum independently of the election of these orbitals. However, in transport one wants to keep the atoms that have matrix elements that enable the transfer of charge with the "external world". This will become clearer later.

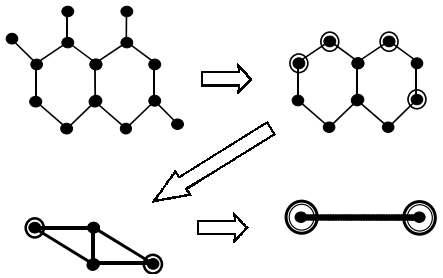

FIG. 7. Sequence of the decimation of a molecule into an effective two site problem.

The spectral and transport properties of model molecules are further discussed in Ref.([15]). Let us mention that the procedure allows to visualize a situation of maximum coupling when $\widetilde{E}_L = \widetilde{E}_R$ which is a resonant situation. This paper also discusses for the first time a situation of maximum decoupling which occurs when $\widetilde{V}_{L,R} = 0$ and was named "antiresonance" or minimal effective decoupling of the centers. This phenomenon is caused by the interference between different pathways when energies of the pathway molecules lie between energies of the other. This generalizes, to the transport case, a concept introduced by Fano[21] in ionization spectroscopy.

G. Advantages of the decimation procedure

One might think that instead of decimating a particular structure one might invert $(\varepsilon\mathbf{I}-\mathbf{H})$ directly. However, there are various advantages in favor of the decimation procedure explained above:

a) The scheme adapts naturally to increase the size of the system without having to recalculate the matrices again.

b) The sparse nature of the Hamiltonian is naturally included in the recursion formula saving storage memory and iteration steps.

c) The decimation scheme has implicit a deep physical insight of the system and reveals the self-similarities of the systems whenever those properties are present.

d) The resulting highly singular resolvent of a big system through matrix inversion is in general numerically unstable. In contrast, the decimation, is a numerically stable procedure. The natural instabilities of the system such as exponentially growing eigensolutions are explicitly used in favor of the convergence of the method. For further discussion on this issue see Ref.[19]. On this basis one establishes that Eq. (52) which defines a Matrix Continued Fraction procedure is more accurate and stable than Eq.(50) which uses a different iteration procedure to calculate an equivalent magnitude.

H. The Thermodynamic limit: Dyson Equation

We have seen that any finite Hamiltonian matrix of finite size can be solved through the decimation method obtaining a set of discrete eigenstates. One might wonder what happens when the number of orbital is actually infinite. How and when does the continuum spectrum appear?. Let's come back to the one-dimensional model. The decimation procedure allows to deal with a simple but already non-trivial case: that of an ordered semi-infinite chain. In this situation: $V_{n,n+1} = V$ and $E_n \equiv E_0$ for every n. The Dyson equation is:

$$\Sigma_n = V\frac{1}{\varepsilon - E_0 - \Sigma_{n+1}}V, \tag{55}$$

and must include the simple fact that every site sees to the right an infinite chain: $\Sigma_n \equiv \Sigma$ for every n. That is a new way to present the Bloch theorem.

$$\Sigma = V\frac{1}{\varepsilon - E_0 - \Sigma}V = \Delta \mp \mathrm{i}\Gamma. \tag{56}$$

The striking fact is that even when we are working with real quantities the solution of this equation may lay in the complex plane[22]. There are two possibilities for the imaginary part. We call retarded self-energy to that which would cause a decay in the time evolution of the wave function amplitude. The solution of the second order equation gives:

$$\Delta = \begin{cases} \frac{\varepsilon-E_0}{2} - \sqrt{\left(\frac{\varepsilon-E_0}{2}\right)^2 - V^2} & \text{if } \varepsilon - E_0 > 2\,|V|\,, \\ \frac{\varepsilon-E_0}{2} & \text{if } |\varepsilon - E_0| \le 2\,|V|\,, \\ \frac{\varepsilon-E_0}{2} + \sqrt{\left(\frac{\varepsilon-E_0}{2}\right)^2 - V^2} & \text{if } \varepsilon - E_0 < -2\,|V|\,, \end{cases} \tag{57}$$

and

$$\Gamma = \begin{cases} 0 & \text{if } |\varepsilon - E_0| > 2\,|V|\,, \\ \sqrt{\left(V^2 - \frac{\varepsilon - E_0}{2}\right)^2} & \text{if } |\varepsilon - E_0| \le 2\,|V|\,. \end{cases} \tag{58}$$

We see that in the region were the Block solutions occur, i.e. when $\varepsilon = E_k \equiv E_0 - 2V\cos(ka)$, is the region where the spectrum is absolutely continuous, one has $\Gamma(\varepsilon) \neq 0$. In the region of the real axis, the Green's functions indetermination represents a branch cut, and it becomes non-analytic at the spectral support. However, the infinite dimensionality of the Hilbert space is a necessary but not sufficient condition for the continuum spectrum. For example, for 1-d systems with disorder in the site energies described by the Anderson model, the self-energies are always real even when the system is infinite i.e. there is genuine "phase transition" in the nature of the states when one goes from finite systems to infinite ones. In an infinite system, disorder can produce a localized-extended transition[23] first described by P. W. Anderson and commonly referred as metal-insulator transition (MIT). The thermodynamic limit that makes possible the study of such transition is to study the observable $\mathcal{O}$ (decay rate, density of states, etc.) in the limit

$$\lim_{\eta\to 0}\lim_{N\to\infty}\mathcal{O}. \tag{59}$$

The order of this limit was implicit when we searched for complex solutions for the Dyson equation by imposing the "Bloch theorem".

We must remember that the MIT is not exclusive to the disordered systems. It is also of frequent occurrence in ordered systems under the action of incommensurate potentials[22]. For example a 1-d systems where the site energy is of the form $E_n = W\cos[Qna]$ with $2\pi/Q$ incommensurate with the lattice length a provided that $W > W_c = 2V$.

I. Density of States in unbounded Systems: Crystals

In the case where the chain extends to both sides of site 0 one gets two contributions to the self energy correction. All diagonal terms of the Green's function are identical

$$\begin{aligned} G^R_{0,0} &= \frac{1}{\varepsilon - E_0 - 2\Sigma^R}, \\ &= \frac{1}{\varepsilon - E_0 - 2\frac{(\varepsilon-E_0)-\mathrm{i}\sqrt{4V^2-(\varepsilon-E_0)^2}}{2}}, \end{aligned} \tag{60}$$

from which the density of states per site (DoS) can be evaluated,

$$N_{[d=1]}(\varepsilon) = \frac{1}{2\pi V}\frac{1}{\sqrt{1-\left(\dfrac{\varepsilon-E_0}{2V}\right)^2}}. \tag{61}$$

which has the characteristic van Hove singularities of one dimensional systems at the band edges.

The fact that the imaginary part in the self-energy is associated to the "irreversible decay" of the state can be formalized by studying the Fourier transform of the Greens function to obtain the return probability

$$\begin{aligned} P_{0,0}(t) &= \left|\langle 0|\exp\left[-\mathrm{i}\mathcal{H}t/\hbar\right]|0\rangle\right|^2 \\ &= \left|\int G^R_{0,0}(\varepsilon)\exp\left[-\mathrm{i}\varepsilon t/\hbar\right]\mathrm{d}\varepsilon\right|^2 \qquad (62) \\ &= |J_0(tV/\hbar)|^2 \sim \frac{1}{\pi}(tV/\hbar)^{-1}. \qquad (63) \end{aligned}$$

where J_0 is the Bessel function. For long times, it represents an irreversible "super-diffusion", and hence differs substantially from a classical random walk process in an infinite chain.

Densities of states in higher dimensions for hyper-cubic lattices can be obtained from those in one dimension by ussing the fact that variables are separable. This allows us to split the energy contributions of each dimension $E(\mathbf{k}) = E_0 + E(k_x) + E(k_y) + E(k_z)$, leading to a convolution expression for the DoS in dimension d=2 and d=3:

$$N_{[2]}(\varepsilon) = \int N_{[1]}(\varepsilon-\varepsilon')\,N_{[1]}(\varepsilon')\,\mathrm{d}\varepsilon' \tag{64}$$

and in general

$$N_{[d+1]}(\varepsilon) = \int N_{[d]}(\varepsilon-\varepsilon')\,N_{[1]}(\varepsilon')\,\mathrm{d}\varepsilon'. \tag{65}$$

For example, in a square lattice we get

$$N_{[2]}(\varepsilon) = \frac{1}{4}K\left[\sqrt{1-(\frac{\varepsilon}{2V})^2}\right], \tag{66}$$

where K is the complete elliptic integral of the first kind. Fig. 8 show the qualitative features of these DoS. See Ref.[24] for a more extended discussions on these points and plots of the DoS in higher dimensions.

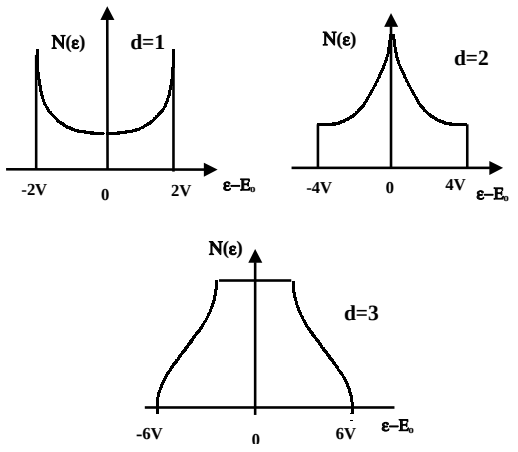

FIG. 8. Schematic Density of States in 1-d, 2-d and 3-d systems.

Now that we know how to evaluate some basic self-energies, we can calculate the Green's function in a great variety of model systems.

J. Surfaces in a semi-infinite chain.

Let us consider the semi-infinite chain $\{s, 1, 2, 3, \cdots\}$. The Green's function at the surface site is

$$G^R_{1,1} = \frac{1}{\varepsilon - E_0 - \Sigma^R(\varepsilon)}, \tag{67}$$

where we have used the subindex 1 for the Green's function to stress on the fact that we count orbitals starting at the surface. One gets the density of states for the surface of the chain

$$N_{surf.}(\varepsilon) = \frac{1}{\pi V}\sqrt{1 - \left(\frac{\varepsilon - E_0}{2V}\right)^2}. \tag{68}$$

Incidentally let us note that an identical DoS is obtained when the Hamiltonian is a Random Matrix[25]. In this case one can use the Lanczos method to tridiagonalize the matrix in the infinite dimension limit and see that it corresponds to the ordered chain we just discussed .

The return probability to the surface site, as defined in Eq.(62) gives

$$P_{1,1}(t) = \left|\frac{\hbar}{Vt}J_1(2Vt/\hbar)\right|^2 \simeq \frac{1}{\pi}\left[\frac{\hbar}{Vt}\right]^3, \tag{69}$$

indicating a decay of the surface state. This exact result, which differs from the usual exponential and diffusive laws usually adopted for the empirical description of decay phenomena, describes an "irreversible" escape from the site. This contrasts with finite systems where recurrences, called mesoscopic echoes[26,27], appear at a typical time estimated as $\hbar/\Delta$, called the Heisenberg time.

Perhaps, the most important conclusion to be drawn from the previous results is the correction to energies of finite systems to account for its contact to infinite systems.

K. Adatoms and Surface states.

The method given above allows us to extend the decimation procedure for finite systems described in the previous section to composite systems (finite +infinite). Let us discuss the simplest but still non-trivial example. Indeed one can think of the 0-th site as an *adatom* in the surface of a metal. In that case its energy E_s and hopping element V_s are different from those of the bulk, E_0 and V respectively. The Green's function evaluation leads to

$$G^R_{s,s} = \frac{1}{\varepsilon - E_s - \left|\frac{V_s}{V}\right|^2 \frac{(\varepsilon - E_0) - \mathrm{i}\sqrt{4V^2 - (\varepsilon - E_0)^2}}{2}}. \tag{70}$$

We leave to the reader the evaluation of the local DoS both numerically and analytically, as well as the calculation of the condition for the appearance of localized states and resonances. For $V_s = V$, a localized state may appear. It shows up as an isolated pole in $G^R_{s,s}(\varepsilon)$ in the real axis at

$$\widetilde{E}_s = \left([E_s - E_0]^2 + V^2\right)/[E_s - E_0], \tag{71}$$

provided that $|-E_0| > 0$.

One can also check that for $|E_s - E_0| < V$ and $\left|\frac{V_s}{V}\right| \ll 1$, a resonant state will appear a pole in the complex plane with a real part overlaping with continuous band. Its energy is:

$$\widetilde{E}_s \simeq E_s + \left|\frac{V_s}{V}\right|^2 \Delta(E_s). \tag{72}$$

The return probability is well approximated by an exponential law as prescribed by the Fermi Golden Rule:

$$P_{s,s}(t) \sim \exp[-t/\tau_s], \tag{73}$$

$$\text{with } \; 1/\tau_s = \frac{2\pi}{\hbar}|V_s|^2 N_{\text{surf.}}(E_s) \simeq 2\Gamma_s(E_s)/\hbar. \tag{74}$$

Again, one sees that the time dependencies that appear in Quantum Mechanics can be very different from those present in a classical random walk.

L. Localized state in a branched circuit.

There is a highly non-trivial result[28] that can be easily obtained with the help of the above formalism. This is the existence of localized states in branching regions.

In general, for a site x to which z semi-infinite chains are connected, the Green's function at the crossing site between branches can be written as

$$G^R_{x,x} = \frac{1}{\varepsilon - E_0 - z\,\dfrac{(\varepsilon - E_0) - \mathrm{i}\sqrt{4V^2 - (\varepsilon - E_0)^2}}{2}}. \tag{75}$$

Which besides of the expected branch cut in $|\varepsilon - E_0| < 2V$, it presents isolated poles at

$$E_{\text{branch}} = E_0 \pm 2V\frac{z^2}{4(z-1)} \tag{76}$$

These solutions, are not only present in a branching polymer, but in a conveniently grown heterostructure[29]. The existence of a topologically confined states in the case $z = 3$ has become the basis for quantum transistors[30] and lasers[31].

M. Representation of the environment through self-energies

First we recall that one can always eliminate microscopic degrees of freedom[16,15] generating an effective Hamiltonian that accounts for them exactly. This produces effective interactions and energy renormalization which depend themselves on the observed energy. Furthermore, one can include the effects of a whole lead in a Hamiltonian description through an *imaginary* correction to the eigenenergies. In fact, an electron originally localized in the region called "the sample" should eventually escape or decay toward the lead. Hence, there is a escape velocity associated with the energy uncertainty of a local state i:

$$v_i = \frac{2a}{\hbar}\Gamma_i = \frac{a}{\tau_i}. \tag{77}$$

Other interactions that one usually considers produce decay rates reasonably well described by the Fermi Golden Rule: electrons in an excited atom decaying into the continuum, or propagating electrons decay into different momentum states by collision with impurities producing phonons or photons. In some of these cases we have to add some degrees of freedom to the sum (the phonon or photon coordinates). A process α may produce a complex contribution ${}^{\alpha}\Sigma_0^R$ which adds into the total self-energy Σ_0^R. In particular this is the interpretation one must give to the small imaginary part η we introduced in the definition of the Green's function of Eq. (29). The effective Hamiltonian becomes:

$$\hat{\mathcal{H}}^{(o)} \xrightarrow[\text{interactions}]{} \hat{\mathcal{H}} = \hat{\mathcal{H}}^{(o)} + \hat{\Sigma}^R, \tag{78}$$

with

$$\hat{\Sigma}^{R(A)} = \sum_i (\Delta_i \mp \mathrm{i}\Gamma_i)(|i\rangle \langle i|\,. \tag{79}$$

That is, we can not find eigenstates because the complete Hamiltonian is not separable into a product of states of the unperturbed system and those of the environment.

In terms of the Green's function the resulting equation is, in the matrix representation:

$$\mathbf{G}^R = \mathbf{G}^{(o)R} + \mathbf{G}^{(o)R}\mathbf{\Sigma}^R\mathbf{G}^R. \tag{80}$$

The diagrammatic expansion for the perturbed Green's function is shown in Fig. 9.

Although the Green's function formalism seems to introduce some extra notation, this has various conceptual advantages. For example, it is straightforward to use Eq.(80) to prove a version of the *optical theorem* which relates the imaginary part of the forward scattering amplitude with the total cross section of the pertubation. One starts by writting Eq. (80) in the form:

$$\mathbf{\Sigma}^R = (\mathbf{G}^{(o)R})^{-1} - (\mathbf{G}^R)^{-1}, \tag{81}$$

and an equivalent one for $\mathbf{\Sigma}^A$. The difference between them is:

$$\begin{aligned}\mathbf{\Sigma}^R - \mathbf{\Sigma}^A &= (\mathbf{G}^A)^{-1} - (\mathbf{G}^R)^{-1}, \\ &= (\mathbf{G}^R)^{-1}\left[\mathbf{G}^R - \mathbf{G}^A\right](\mathbf{G}^A)^{-1},\end{aligned} \tag{82}$$

from which we obtain:

$$\left[\mathbf{G}^R - \mathbf{G}^A\right] = \mathbf{G}^R\ \left[\mathbf{\Sigma}^R - \mathbf{\Sigma}^A\right]\ \mathbf{G}^{\mathbf{A}}, \tag{83}$$

which has deep physical significance. It is an integral equation relating the local densities of states given Eq.(36) and the decay rates provided by Eq. (77). Perhaps, the most important advantage of Green's functions, is that they can be used also in the Quantum Field Theory[32,33] to deal with the many-body case and are a relevant tool in the clarification of the problem of tunneling time.

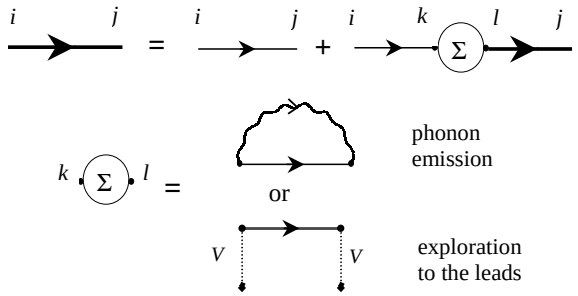

FIG. 9. Diagrams shown before can be rearranged into the self-energy correction Σ. This equation is valid for independently of the approximation used to calculate Σ. In the lower panel self-energies obtained through escape to the leads and electron-phonon interactions are shown. The escape self-energies contain the hopping (dot) and a propagator in the lead. An electron-phonon self-energy is evaluated in terms of the sample's electron (straight-line) and phonon (wavy-curve) Green's functions.

IV. THE FISHER AND LEE FORMULA

The original demonstration[34] of the connection between transmittance and Green's function is based on properties of the scattering matrix in the continuum model. It is also presented in a simplified form in the book by Datta[35]. Here we are going to present the main lines of a demonstration based on properties of a molecular orbital model in its decimated tight binding version.

The isolated sample can be decimated into two sites getting an exact non-linear effective Hamiltonian:

$$\hat{\mathcal{H}}_0 = E_1 \left|1\right\rangle \left\langle 1\right| + E_N \left|N\right\rangle \left\langle N\right| + V_{1,N} \left|1\right\rangle \left\langle N\right| + V_{N,1} \left|N\right\rangle \left\langle 1\right|, \tag{84}$$

where the parameters E and V are functions of the variable ε.

We attach electrodes or leads at each site. Both leads are perfect semi-infinite 1-d chains where the dispersion relations are

$$E_{kL} = E_L + 2V_L \cos[k_L a], \tag{85}$$

from which the group velocity is

$$v_L = \frac{1}{\hbar}\frac{\partial E_{kL}}{\partial k_L} = -\frac{2aV_L}{\hbar}\sin[k_L a]. \tag{86}$$

Analogous relations for E_{kR} and v_R hold in the right channel. When the perturbation

$$\hat{\mathcal{H}}_{0-\text{leads}} = V_{tL}(\left|1\right\rangle \left\langle 0\right| + \left|0\right\rangle \left\langle 1\right|) + V_{tR}(\left|N\right\rangle \left\langle N+1\right| + \left|N+1\right\rangle \left\langle N\right|) \tag{87}$$

is turned on, the new single particle eigenfunctions components

$$u_k(an) = \begin{cases} \exp[\mathrm{i}kna] + r\exp[-\mathrm{i}kna] & \text{if } \ n \leq 0, (na \in L), \\ A & \text{if } \ n = 1, \\ B & \text{if } \ n = N, \\ t\exp[\mathrm{i}kna] & \text{if } \ n \geq N+1, (na \in R), \end{cases} \tag{88}$$

are determined from the stationary Schrödinger equation $\left(\varepsilon\hat{\mathcal{I}} - \hat{\mathcal{H}}\right)\left|\psi\right\rangle = 0$. We have only four non trivial terms which contain either A or B. One eliminates A, B and t and evaluates

$$T_{R,L} = 1 - r^* r \tag{89}$$

$$= 4\left|\frac{V_{tL}}{V_L}\right|^2 (|V_L|\sin\left[k_L a\right])\left|V_{1,N}\right|^2 \left|\frac{V_{tR}}{V_R}\right|^2 (|V_R|\sin[k_R a])/[dd^*], \tag{90}$$

where

$$\begin{aligned} d = & \left[\varepsilon - E_1 + \left|\frac{V_{tL}}{V_L}\right|^2 \{|V_L|\cos[k_L a] - \mathrm{i}\,|V_L|\sin[k_L a]\}\right] \\ & \times \left[\varepsilon - E_N + \left|\frac{V_{tR}}{V_R}\right|^2 \{|V_R|\cos[k_R a] - \mathrm{i}\,|V_R|\sin[k_R a]\}\right] \\ & - \left[V_{1,N}V_{N,1}\right]. \end{aligned}$$

In order to compare this with the Green's function we remember that the effective site energies include the self-energies produced by the leads

$$\begin{aligned} {}^L\Sigma_1 &= \left|\frac{V_{tL}}{V_L}\right|^2 (|V_L|\cos[k_L a] - \mathrm{i}\,|V_L|\sin[k_L a]) \\ &= {}^L\Delta_1 - \mathrm{i}\ {}^L\Gamma_1, \end{aligned} \tag{91}$$

and

$$\begin{aligned} {}^R\Sigma_1 &= \left|\frac{V_{tR}}{V_R}\right|^2 (|V_R|\cos[k_R a] - \mathrm{i}\,|V_R|\sin[k_R a]) \\ &= {}^R\Delta_N - \mathrm{i}\ {}^R\Gamma_N. \end{aligned} \tag{92}$$

If the lead variables are decimated they produce an effective potential of the form

$$\hat{\mathcal{H}}_{\text{eff.}} = \hat{\mathcal{H}}_0 + {}^L\Sigma_1 \left|1\right\rangle \left\langle 1\right| + {}^R\Sigma_N \left|N\right\rangle \left\langle N\right|.$$

This maintains the structure of an effective two site Hamiltonian. From this it is simple to compute the four components of the exact Green's function of the system

$$\begin{aligned} G^R_{1,N} &= \left\langle 1\right| \left[\varepsilon\hat{\mathcal{I}} - \hat{\mathcal{H}}_{\text{eff.}}\right]^{-1} \left|N\right\rangle \\ &= \frac{V_{1,N}}{\left[\varepsilon - \left(E_1 + {}^L\Sigma_1^R\right)\right]\left[\varepsilon - \left(E_N + {}^R\Sigma_N^R\right)\right] - V_{1,N}V_{N,1}} \end{aligned} \tag{93}$$

obtaining the Fisher-Lee formula

$$T_{R,L}(\varepsilon) = \left(\frac{\hbar}{a}\right)^2 v_R\, v_L G^R_{R,L}(\varepsilon)\, G^A_{L,R}(\varepsilon). \qquad (94)$$

Originally, Fisher and Lee considered only the escape velocity to the leads (i.e. $\alpha = \beta =$ lead). D'Amato and Pastawski[36] were the first to realize that because of Eq. (86) one could write transmittances in terms of the imaginary part of the self energies. Immediately, our point is that *any other process* which contributes to decay *giving an imaginary* contribution to the *self-energy* would be described by Eq. (94). In particular, this will be true for a "decoherence" velocity as would be the case of the electron-phonon rate described in the previous section. In a modern notation:

$$T_{\alpha R,\beta L}(\varepsilon) = \left[2\,{}^{\alpha}\Gamma_R(\varepsilon)\right]\, G^R_{\alpha R,\beta L}(\varepsilon)\, \left[2\,{}^{\beta}\Gamma_L(\varepsilon)\right] G^A_{\beta L,\alpha R}(\varepsilon). \qquad (95)$$

The left supra-index in Γ indicates the process or channel associated to the electron decay from the spatial region identified with the right subindex. Both indices appear as sub-indices in the Green's function. Notice that ${}^{\beta}\Gamma_L(\varepsilon)$, which corresponds to the interaction with the "source" of particles, was arranged between two Green's functions. ${}^{\alpha}\Gamma_R(\varepsilon)$, representing the properties of the "sink", was placed at left. This order is important in the matrix representation.

A. An example: branched circuit.

In order to apply the Fisher-Lee formula to a simple but highly non-trivial example, let us consider again the circuit with z equivalent branches. One might think that a plane wave incoming at the node from one of the branches will have a probability $1/(z-1)$ to be transmitted to each of the others, i.e. that it will behave as a perfect $(z-1)$-splitter. The true answer comes from the quantum evaluation giving

$$T = \frac{4}{z^2}\frac{1}{1+(\frac{2-z}{z})^2\dfrac{(\varepsilon-E_0)^2}{(4V)^2-(\varepsilon-E_0)^2}}. \qquad (96)$$

T has a maximum of $4/z^2$, lower than the classical value. Additionally, the transmittance goes to zero as the energy approaches the band edge. This is due to the presence of the localized state found in Eq. (76) which precludes the occupation of the branching region by the propagating states.

B. An extension: the multichannel case.

In fact, one can see that it is not difficult to generalize Eq. (4) to any number of incoming and outgoing channels connected to their respective reservoirs. When the two wires L and R have finite cross section, each wire contains an integer number, ${}^{L}M_{(\varepsilon_F)}$ and ${}^{R}M_{(\varepsilon_F)}$, of propagating (one-dimensional) channels (i.e. transversal modes) allowed by the Fermi energy. Each electronic excitation leaving the wire L in the propagating channel i with velocity $v_{Li} \neq 0$, enters the wire R in the propagating channel j with velocity $v_{Rj} \neq 0$. The conductance in the linear response regime is

$$\mathsf{G}_{R,L} = \frac{e^2}{h}\sum_{\alpha\in L}^{{}^{L}M}\sum_{\beta\in R}^{{}^{R}M} T_{\beta,\alpha}. \qquad (97)$$

This can be written by combining Eqs. (95) and (97)into a compact matrix notation:

$$\mathsf{G}_{R,L} = \frac{e^2}{h} 4\ \mathrm{Tr}\left[\mathbf{\Gamma}_R(\varepsilon)\,\mathbf{G}^R_{R,L}(\varepsilon)\mathbf{\Gamma}_L(\varepsilon)\,\mathbf{G}^A_{L,R}(\varepsilon)\right]. \qquad (98)$$

The sum of initial states at left is the result of the product of the diagonal form of the broadening matrix $\mathbf{\Gamma}_L(\varepsilon)$, while the trace corresponds to the sum over final states.

V. APPLICATIONS OF LANDAUER'S COHERENT CONDUCTANCE

A. Lyapunov Exponents and Localization Length.

The calculation of actual eigenstates in disordered potentials of an infinite system is a very subtle mathematical problem. In contrast, the computation of Green's functions and conductances of arbitrary size can be done at a relatively low computational cost. The sparse nature of the single particle Hamiltonian when it is expressed in a localized basis (tight-binding approximation) allows the implementation of a recursive calculation of the Green's function. These methods, originally devised to deal with inhomogeneous and disordered systems, allow the calculation of the quantum transmittances such as $T_{R,L}$. Typically, it requires L_x/a operations (products and inversions) with matrices of size $M \times M$.

Historically, Landauer's reasonings were decisive in the development of the theory of electronic localization in disordered systems[19,23]. In particular, the method developed above can be used to proof rigorously that in one dimension there are no extended states. Every eigenstate should decay exponentially away of some particular localization center. The exponential rate corresponds to the Lyapunov exponent γ of the iterative Dyson Equation. The associated length, $\xi = 1/\gamma$, is called localization length.

The Lyapunov exponent can be evaluated from the Green's functions $G_{1,n}$ and $G_{n,n}$ using the limit relations

$$\gamma(\varepsilon) = \frac{1}{a}\lim_{L\to\infty}\left[\frac{1}{L}\ln\left|\frac{G_{L,L}(\varepsilon)}{G_{1,L}(\varepsilon)}\right|\right]. \qquad (99)$$

This definition is completely general and works either for ordered and disordered situations. To check how it works, let us first consider the 1-d *ordered chain*. The solution of Eq. (99) is analytic

$$\gamma(\varepsilon) = \begin{cases} \frac{1}{a}\text{arccosh}\left[\dfrac{\varepsilon - E_0}{2V}\right] & \text{for } |\varepsilon - E_0| > |2V|\,, \\ 0 & \text{for } |\varepsilon - E_0| < |2V|\,. \end{cases} \tag{100}$$

This clarifies that $\gamma(\varepsilon)$ is just the analytical continuation of the wave vector $k(\varepsilon)$. Already in this case, we can identify two regions: one which coincides with the Bloch band where localization length is infinite and the rest, where the states, if any, are localized. This is the region where the described states in the branching region and the surface states lie.

B. Localization in a Conjugated Polymer.

In order to consider a more realistic example of specific interest in molecular electronics, let us consider a model[6] for the simplest conjugated polymer: polyacetilene. This can be described by the Hamiltonian,

$$\hat{\mathcal{H}}_0 = \sum_{n(\text{odd})} \{V_2 \,|n\rangle \langle n+1| + V_1 \,|n+1\rangle \langle n+2| + \text{c.c.}\}\,, \tag{101}$$

where $V_2 = -(V_\pi + \delta)$ and $V_1 = -(V_\pi - \delta)$ where $V_\pi > 0$ is the energy associated with a $\pi - \pi$ bonding. This is represented schematically in Fig.10. δ is the additional energy involved in the dimerization to form the alternate double bond (conjugated system). Hence, the unit cell has two C-H monomers. Again, the Lyapunov exponent can be calculated either analytically or numerically giving

$$\gamma(\varepsilon) = \begin{cases} \frac{1}{a}\text{arccosh}\left[\frac{\varepsilon^2 - ({V_1}^2 + {V_2}^2)}{2V_2 V_1}\right] \text{at the gaps} \\ 0 \text{at the valence band}, V_2 + V_1 < \varepsilon < V_2 - V_1 \\ 0 \text{at the conduction band}, -V_2 + V_1 < \varepsilon < -V_2 - V_1. \end{cases} \tag{102}$$

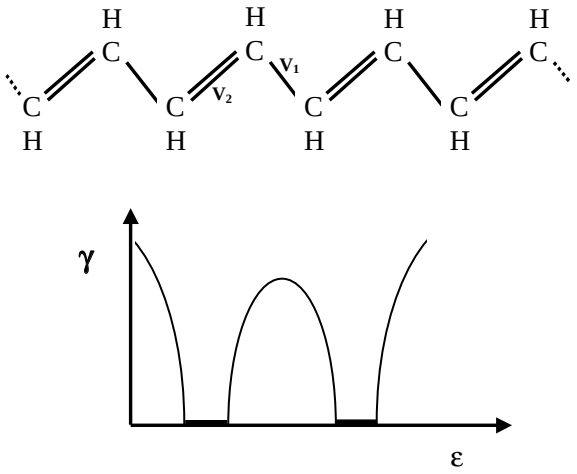

FIG. 10. In the upper panel the polyacetilene macromolecule is represented. Double bonds and simple bonds alternate. This gives an alternation in the energies associated to π-π bonding. The lower scheme is the Lyapunov exponent as a function of the energy. Scales are discussed in the text.

This simple situation hints at the solution of a the more complex disordered systems. Conceptually, a disordered sample can be visualized as a periodic array of disordered unit cells of size $L = Na$, with a progressively increasing N. Then, the localization transition appears as the dominance of the "gaps" over the "bands" whose width (spectral support) decreases as $V \exp[-\gamma Na]$. With the decimation methodology developed above, the numerical evaluation of the Lyapunov exponent is straightforward.

C. Metal-Insulator Transition.

In one dimensional systems, the exponential decrease of the conductance follows directly from the statistical properties of the transmission probability $T \sim \exp\left[-L_x/\xi\right]$ in a disordered system. Therefore, the 'four-probe ' Landauer's conductance given by Eq. (5), by describing the intrinsic properties of the "sample", contains the correct scaling behavior of the conductance ranging from the non-extensive behavior when $L_x \gg \xi$,

$$\mathsf{G}^{\text{f.p.}}_{R,L}(L_x) \simeq \frac{e^2}{h} \exp\left[-L_x/\xi\right], \tag{103}$$

to the expected Ohmic behavior described by Drude's law in terms of the mean free path $\ell = \xi/2$,

$$\mathsf{G}^{\text{f.p.}}_{R,L}(L_x) = e^2 N_0 \, v_F \, \ell / L_x, \tag{104}$$

when $L_x < \ell$. Statistical subtleties aside, this last result is obtained by expanding the transmittance in its lowest order in L_x/ξ.

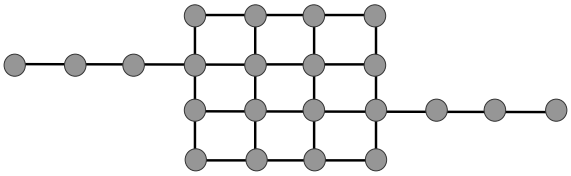

FIG. 11. Scheme of the use of the calculation of 1-d transmittance to obtain the transport properties of a 2-d system.

A similar reasoning can be applied to higher dimensional systems ($d \geq 2$) with hyper-cubic shape. The conductance can be calculated with Eq.(5) by attaching two one-dimensional leads. The metal-insulator transition is possible because the curve $\xi(L) = 2\ell(L/a)^{d-1}$, valid for weak scattering, bends down to an asymptotic value $\xi(L) \to \xi_\infty$. This effect manifests itself in a universal behavior. One considers the conductance of samples of size $L^d = (Na)^d$ with Anderson disorder with two one dimensional leads attached as shown in Fig.11. The adimensional conductance $g_L = \frac{h}{e^2}\mathsf{G}^{\rm f.p.}_{R,L}(L)$ is calculated using Eq.(5). For each dimensionality, all sizes and disorders strength scale into a single scaling curve

$$\beta_d = \frac{L}{g_L}\frac{\mathrm{d}g_L}{\mathrm{d}L}. \tag{105}$$

This is shown in Fig.12 for dimensions $d = 2$ and $d = 3$ as a function of $\ln[g_L]$.

The arrows indicate the directions in which g_L moves as the size of the system increases. The fact that $\beta_{d=2}$ (full circles) flows from $\beta_2 = 0$ towards $-\infty$ indicates that, for any positive disorder all states are localized. In contrast, in a $\beta_{d=3}$ the curve can flow either towards $\beta_2 = 1$, if the disorder is weak enough ($W < W_c$), or towards $\beta_2 \to -\infty$ for disorder above certain critical value ($W > W_c$ with $W_c \simeq 6.5V$). This shows that the MIT is a critical phenomenon as any other thermodynamical phase transition.

The point we want to stress here is that the "non-invasive voltage probes" of the Landauer picture rescue a "local" meaning for the conductance and emphasizes the non-extensive behavior introduced by quantum interferences. The presence of decoherent processes or voltmeters on a scale L_ϕ "break" the quantum conductance into an incoherent sum of $\frac{L_\phi}{L_x}$ separate pieces where the transport is coherent and hence described by Eq. (5). The total conductance becomes $\mathsf{G}_{R,L}(L_x) = \frac{L_\phi}{L_x}\mathsf{G}^{\rm f.p.}_{R,L}(L_\phi)$ recovering the extensive Ohmic behavior.

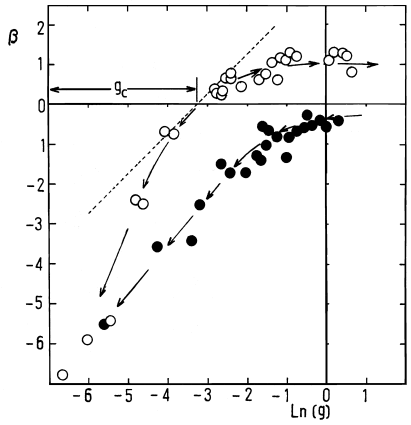

FIG. 12. Numerical scaling function $\beta = (L/g_L)(\Delta g_L/\Delta L)$ evaluated from the adimensional conductance g_L of samples of 2-d and 3-d system size L^d. We use the Anderson model at $\varepsilon_F = 0$. Data for disorder $W/V = 4, 5, 6, 7, 8, 10, 14$ and sizes up to $L^2 = 20 \times 20a^2$ collapse in the 2-d curve of the filled circles. Data for disorder $W/V = 6, 8, 10, 14, 15.5, 16.5, 17$ and 18 and sizes up to $L^3 = 6\times6\times6a^3$ collapse in the 3-d curve of the empty circles. In 3-d the critical conductance is $g_c \simeq 3.2$ and corresponds to a critical disorder $W_c/V \simeq 16$.

D. The Aharonov-Bohm effect and non-local properties.

Setting the Zeeman effect aside, the main consequence of a magnetic field is to affect the wave function's phase in

$$\phi = \frac{e}{hc}\int \vec{A}\cdot\mathrm{d}\vec{l}.$$

In the Peierls substitution, appropriate for discrete models, this is achieved by modifying the coupling $V \mapsto V\exp[\mathrm{i}\phi]$.

When we have a system[37] as that shown in Fig.13, the application of the magnetic field will result in an oscillation of the conductance[38] due to the interference of the probability amplitudes propagated through different branches of the system.

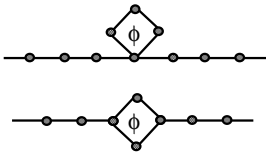

FIG. 13. Two tight binding representations of path loops affecting the conductance in a non-local fashion as discussed in the text.

Let's assume that in absence of field these pathways superpose in the form of maximally destructive interference in the forward direction and have constructive probability of return $P_{0,0}$ (this is localization)

$$P_{0,0} = \left| \sum_{i(\text{paths})} u_0^i \right|^2 = \sum_i \left| u_0^i \right|^2 + \sum_{i \neq j} u_0^i u_0^{j*} \qquad (106)$$

The first term in the right side is the contribution of uncorrelated pathways. The second term gives the interference effects, it is affected by the magnetic field and contains the non-local effects intrinsic to the Schrödinger equation. In presence of a gauge field A, destructive interference is modified producing an increase of the transmittance. This is a positive magnetoconductance[39], a characteristic effect of coherent systems at very low fields. If the inelastic events along the pathways start contributing to the loss of phase memory, the field effect becomes progressively weaker until it eventually disappears. As we will see bellow, a very strong magnetic field causes interferences in the short distances (toward the Landau levels) therefore giving a new tendency toward localization.

E. Conductance quantization in 2-d

Extending what is observed in a 1-d ordered chain, where transmittances are either 0 or 1 depending on the energy of the injected excitation; when one considers the 1^+-d (strips) and real 2-d systems, we have to account for the different propagating modes. As the available energy increases, new lateral modes becomes available increasing the total current. According to Eq. (97) the conductance is bounded by

$$\mathsf{G}_{R,L} \leq \frac{e^2}{h} \min[{}^L M_{(\varepsilon_F)}, {}^R M_{(\varepsilon_F)}]. \qquad (107)$$

For perfect transmitting samples, a situation that requires order and reflection symmetry (${}^L M_{(\varepsilon_F)} = {}^R M_{(\varepsilon_F)}$), $T_{j,i}$ is either 1 or 0 and one obtains the conductance quantization in integer multiples of e^2/h. This effect is spectacularly verified in specially tailored nanostructures. The conductance's discrete steps are shown in Fig.14.

Such an effect is restricted to artificial devices[40]. The same effect occurs when there is a metallic bridge between two electrodes and these are pulled apart. The bridge stretches becoming progressively thinner until its breakdown. This process is monitored by the carriers, which, as the bridge becomes narrower, loose propagating channels below the Fermi energy. As a consequence the conductance shows clear steps such as those shown in in Fig.14. The adiabatic approximation, justified by the high electronic speeds as compared to any modification of the contact structure, allows the use of a simple model where the time is parametrically associated with the width represented in Fig.15.

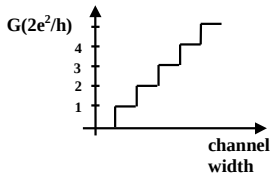

FIG. 14. Quantized conductance as a function of channel width.

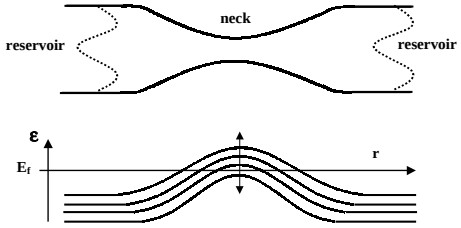

FIG. 15. Geometry of neck formed when a nanowire is pulled lengthwise. As the transverse dimension shrinks conductance channels are excluded as shown in the lower panel where we show a scheme of the transversal modes energies as a function of position.

F. Hall Effect

In the classic theory of the Hall effect the external magnetic field produces a coefficient $R_H = -1/ne$ which is negative if the carriers are electrons and is inversely proportional to the electron density. In a two dimensional system, we can evaluate the Hall effect at low fields by using a simple model that has two 1-d contacts to inject and measure the current and two additional ones to measure the Hall voltage. These are shown in Fig.16

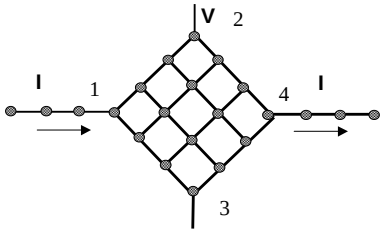

FIG. 16. Geometrical representation of the model used to evaluate the Hall effect.

Since the chemical potentials and voltages are related by $\mathsf{V}_p = \mu_p/e$, Eq.(7) becomes

$$\mathsf{I}_p = \sum_{q=1}^{4} [\mathsf{G}_{q,p}\mathsf{V}_p - \mathsf{G}_{p,q}\mathsf{V}_q].$$

When all the chemical potentials are equal, there is no current and $\sum_q \mathsf{G}_{p,q} = \sum_p \mathsf{G}_{q,p}$ from which

$$\mathsf{I}_p = \sum_{q=1}^{4} \mathsf{G}_{p,q}(\mathsf{V}_p - \mathsf{V}_q).$$

We can always choose one of the voltages, e.g. one of the current leads as a reference setting $\mathsf{V}_4 = 0$. Therefore, the problem simplifies to three linear equations

$$\begin{pmatrix} \mathsf{I}_1 \\ \mathsf{I}_2 \\ \mathsf{I}_3 \end{pmatrix} = \begin{pmatrix} \mathsf{G}_{2,1} + \mathsf{G}_{3,1} + \mathsf{G}_{4,1} & -\mathsf{G}_{1,2} & -\mathsf{G}_{1,3} \\ -\mathsf{G}_{2,1} & \mathsf{G}_{1,2} + \mathsf{G}_{3,2} + \mathsf{G}_{4,2} & -\mathsf{G}_{2,3} \\ -\mathsf{G}_{3,1} & -\mathsf{G}_{3,2} & \mathsf{G}_{1,3} + \mathsf{G}_{2,3} + \mathsf{G}_{4,3} \end{pmatrix} \begin{pmatrix} \mathsf{V}_1 \\ \mathsf{V}_2 \\ \mathsf{V}_3 \end{pmatrix}.$$

In short $\mathsf{I}_i = \sum_j M_{i,j}\mathsf{V}_j$, where we invert the matrix of conductances $\mathbf{M}$ obtaining

$$\begin{pmatrix} \mathsf{V}_1 \\ \mathsf{V}_2 \\ \mathsf{V}_3 \end{pmatrix} = \begin{pmatrix} \mathsf{R}_{1,1} & \mathsf{R}_{1,2} & \mathsf{R}_{1,3} \\ \mathsf{R}_{2,1} & \mathsf{R}_{2,2} & \mathsf{R}_{2,3} \\ \mathsf{R}_{3,1} & \mathsf{R}_{3,2} & \mathsf{R}_{3,3} \end{pmatrix} \begin{pmatrix} \mathsf{I}_1 \\ \mathsf{I}_2 \\ \mathsf{I}_3 \end{pmatrix}.$$

Let's see one of its elements,

$$\mathsf{R}_{1,1} = \frac{(\mathsf{G}_{2,3} + \mathsf{G}_{2,4} + \mathsf{G}_{2,1})(\mathsf{G}_{3,1} + \mathsf{G}_{3,2} + \mathsf{G}_{3,4}) - \mathsf{G}_{2,3}\mathsf{G}_{3,2}}{\det[\mathbf{M}]}.$$

The voltage between 2 and 3 is related to the total current

$$\mathsf{R}_\mathsf{H} = \frac{\mathsf{V}}{\mathsf{I}} = \frac{\mathsf{V}_2 - \mathsf{V}_3}{\mathsf{I}_1} = \mathsf{R}_{2,1} - \mathsf{R}_{3,1}$$

which will be zero in absence of a magnetic field. Otherwise, the dependence on magnetic field implicit in the quantum mechanical evaluation of $\mathsf{R}_{2,1}$ and $\mathsf{R}_{3,1}$, gives the Hall resistance.

There are certain symmetry relations that should be obeyed on the basis of the so called Onsager-Casimir relations; in the linear response regime the Hall resistance obeys

$$\mathsf{R}_H(B) = -\mathsf{R}_H(-B), \tag{108}$$

where B is the applied field. The previous relation involves the minus sign because the Hall voltage is reversed in the field. Nevertheless, if one simultaneouly exchanges the voltage probes there is no change. On the other hand the ordinary longitudinal resistance does not change under the reversal of the field. The symmetry relation can be summarized as

$$\mathsf{R}_{xx}(B) = \mathsf{R}_{xx}(-B), \tag{109}$$

and

$$\mathsf{R}_{xy}(B) = \mathsf{R}_{yx}(-B). \tag{110}$$

These symmetries are well satisfied for an homogeneous sample. On the other hand, for inhomogeneous samples no specific symmetry is experimentally found upon reversing the field. This is due to irregular current patterns occuring in the sampple mixing both xx and xy components the first one being symmetric, and the second antisymmetric, in the field. A more general relatioship for a four probe device can be given as follows: if one defines the resistance $\mathsf{R}_{mn,kl}$ as that taken when measuring the voltage between probes k, l while putting current I between probes m, n (imput at m output at n)

$$\mathsf{R}_{mn,kl} = \frac{\mathsf{V}_\mathsf{k} - \mathsf{V}_\mathsf{l}}{I}. \tag{111}$$

The *reciprocity relations* are then expressed as

$$\mathsf{R}_{kl,mn}(B) = \mathsf{R}_{mn,kl}(-B). \tag{112}$$

The Integer Quantum Hall Effect IQHE[41] follows from the use of Eq. 7 in the condition that strong magnetic fields confine the propagating electrons to the sample boundaries. The appearance of these new spatial selection rules precludes backward scattering and decoherence[42], yielding the unitary transmittances responsible for the IQHE.

VI. DECOHERENCE IN QUANTUM TRANSPORT

A. Phenomenology

It is obvious that because of the experimental limits for the coherent description introduced above one should observe[43] important departures from those predictions. A first alternative to include decoherence in quantum transport was inspired by the Landauer's formulation. There, the leads, while accepting a quantum description of their spectra and their ability to propagate excitations, are the ultimate source of irreversibility and decoherence: Electrons leaving the leads toward the sample are completely incoherent with the electrons coming from the other leads (see Fig. 17). In fact, it is obvious that a wire connected to a voltmeter, by "measuring" the number of electrons in it, must produce some form of collapse of the wave function leading to decoherence.

Besides, no net current flows toward a voltmeter. Leads are then a natural source of decoherence which can be readily described in the Landauer's picture if one uses the Landauer conductances together with the Kirchhoff balance equations. This fact was firstly realized by M. Büttiker[44]. The procedure, resulting from the application of Kirchhoff law to each lead, is called the Landauer-Büttiker equation[14]. Let us see how it works for the case of a single voltmeter. In matrix form

$$\begin{pmatrix} \mathsf{I}_L \\ \mathsf{I}_\phi \\ \mathsf{I}_R \end{pmatrix} = \begin{pmatrix} -[\mathsf{G}_{R,L}+\mathsf{G}_{\phi,L}] & \mathsf{G}_{L,\phi} & \mathsf{G}_{L,R} \\ \mathsf{G}_{\phi,L} & -[\mathsf{G}_{R,\phi}+\mathsf{G}_{L,\phi}] & \mathsf{G}_{\phi,R} \\ \mathsf{G}_{R,L} & \mathsf{G}_{R,\phi} & -[\mathsf{G}_{\phi,R}+\mathsf{G}_{L,R)} \end{pmatrix} \begin{pmatrix} \mathsf{V}_L \\ \mathsf{V}_\phi \\ \mathsf{V}_R \end{pmatrix}. \tag{113}$$

Here, the unknowns are $\mathsf{I}_L, \mathsf{I}_R$ and $\mathsf{V}_\phi = \delta\mu_\phi/e$. The second equation must be solved with the voltmeter condition $I_\phi \equiv 0$

$$0 = \frac{e}{h}T_{\phi,L}(\delta\mu_\phi - \delta\mu_L) + \frac{e}{h}T_{R,\phi}(\delta\mu_\phi - \delta\mu_R), \tag{114}$$

yielding us $\delta\mu_\phi$ to be introduced in the third equation

$$\mathsf{I}_R = \frac{e}{h}T_{R,L}(\delta\mu_L - \delta\mu_R) + \frac{e}{h}T_{R,\phi}(\delta\mu_L - \delta\mu_\phi) \tag{115}$$

to obtain the current at the voltage source

$$\mathsf{I}_R = \frac{e}{h}\widetilde{T}_{R,L}(\delta\mu_L - \delta\mu_R) \tag{116}$$

with

$$\widetilde{T}_{R,L} = T_{R,L} + \frac{T_{R,\phi}T_{\phi,L}}{T_{R,\phi}+T_{\phi,L}}. \tag{117}$$

The first term can be identified with the coherent part, while the second is the incoherent or sequential, i.e. the contribution to the current originated from particles coming from the voltmeter. This corresponds to an effective conductance of

$$\widetilde{\mathsf{G}}_{R,L} = \mathsf{G}_{R,L} + (\mathsf{G}_{R,\phi}{}^{-1} + \mathsf{G}_{\phi,L}{}^{-1})^{-1}, \tag{118}$$

which can be identified with the electrical circuit of Fig. 18. This classical view clarifies the competition between coherent and incoherent transport. What this circuit does not hint at is that in Quantum Mechanics one cannot modify one of the resistances without deeply altering the others.

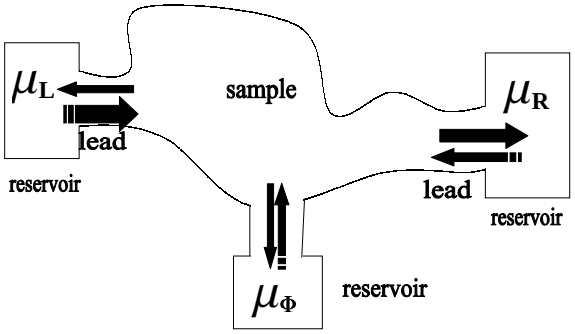

FIG. 17. Representation of a three probe measurement. The volt-meter may be strongly coupled and is a source of decoherence.

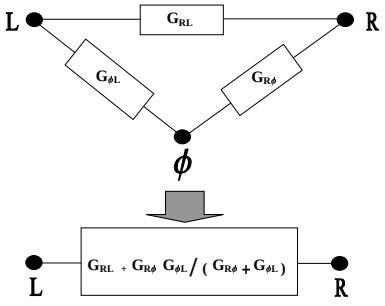

FIG. 18. Classical circuit representation of the non-classical system with quantum coherent and incoherent transport. The coherent component is a direct resistance between left (L) and right (R) electrodes. Quantum mechanics makes these effective resistances interdependent.

So far with the phenomenology. The next important step is to connect these quantities with actual model Hamiltonians. This connection was made explicit by the contribution of D'Amato and Pastawski[36](DP).

B. The D'Amato-Pastawski model for decoherence.

The DP model refers to a simple way to account for the infinite degrees of freedom of the thermal bath or the electron reservoirs. This follows from our general approach: to obtain exact solutions to simple problems instead of finding approximate solutions of complex problems. Let us first review the basic mathematical background that made possible the selection of a simple Hamiltonian that best represents the complex sample-environment system. The objective was to use its exact solution in the Landauer's transport equation. Here, we describe the DP model for decoherence and show how it applies to a simple resonant tunneling system. Consider the sample's Hamiltonian

$$\hat{\mathcal{H}}_0 = \sum_{i=1}^{N} \left\{ E_i \left|i\right\rangle \left\langle i\right| + \sum_{j=1(\neq i)}^{N} V_{i,j} \left[\left|i\right\rangle \left\langle j\right| + \left|j\right\rangle \left\langle i\right| \right] \right\}, \tag{119}$$

where i and j indicate sites on a lattice. Notice that interactions are not restricted to nearest neighbors. However, for the usual short range interactions, the Hamiltonian matrix has the advantage of being sparse. The local dephasing field is represented by

$$^{\phi}\hat{\Sigma}^{R} = \sum_{i}^{N} -(\mathrm{i}\ )^{\phi}\Gamma\ \ \left|i\right\rangle \left\langle i\right|, \tag{120}$$

where $^{\phi}\Gamma = \hbar/(2\tau_{\phi})$ and we consider for simplicity only two one-dimensional current leads L and R connected at sites 1 and N respectively

$$^{\text{leads}}\hat{\Sigma}^{R} = -\mathrm{i}\left({}^{L}\Gamma\ \left|1\right\rangle \left\langle 1\right| + \ {}^{R}\Gamma\ \ \left|N\right\rangle \left\langle N\right| \right). \tag{121}$$

We see that the 1st site has escape contributions towards *both*, the current lead at the left, $^{L}\Gamma_1$, *and* the inelastic channel associated to this site, $^{\phi}\Gamma_1$. The on-site chemical potential will ensure that no net current flows through the latter channel.

C. The solution for incoherent transport

The adimensional conductances are just the transmission probabilities. In principle, they can be computed in terms of the Green's function according to Eq. (95). To simplify the notation we define the total transmission from each site as

$$(1/g_i) \equiv \sum_{j=0}^{N+1} T_{j,i} = \begin{cases} 4\pi N_1\ {}^{L}\Gamma_1 & \text{for } i = 0 \\ 4\pi N_i\ {}^{\phi}\Gamma_i & \text{for } 1 \leq i \leq N \\ 4\pi N_N\ {}^{R}\Gamma_N & \text{for } i = N+1 \end{cases} \tag{122}$$

The last equality follows from the optical theorem. The balance equation becomes

$$\mathsf{I}_i \equiv 0 = -\left(1/g_i\right)\delta\mu_i + \sum_{j=0}^{N+1} T_{i,j}\delta\mu_j, \tag{123}$$

where the sum adds all the electrons that emerge from a last collision at other sites (j's) and propagate coherently to site i. These include the electrons coming from the current source i.e. $T_{i,L}\delta\mu_L$ and the current drain. However, since we refer all voltages to the last one, $T_{i,R}\delta\mu_{R.} \equiv 0$. We remark that here we do not exclude the i-th site from the summations in Eqs. (123) and (122). While this has no consequences in the steady state, they become relevant in the time dependent formulation. To fix the physical interpretation we emphasize that the last term accounts for the electrons that emerging from a dephasing collision at site j will propagate coherently to site i where they have a dephasing collision. The first term accounts for all the electrons that emerge from this collision on site i to have a further dephasing collision either in the sample or in the leads. The net current is identically zero at any dephasing channel ("lead"). The other two equations are

$$\mathsf{I}_L \equiv -\mathsf{I} = -\left(1/g_i\right)\delta\mu_L + \sum_{j=0}^{N} T_{i,j}\delta\mu_j, \tag{124}$$

$$\mathsf{I}_R \equiv \mathsf{I} = -\left(1/g_i\right)\delta\mu_i + \sum_{j=0}^{N+1} T_{i,j}\delta\mu_j.$$

Here, we need the local chemical potentials. They can be obtained from Eq. (123). In a compact notation, these coefficients can be arranged in a matrix form which excludes the leads that are current source and sink

$$\mathbf{W} = \begin{pmatrix} T_{1,1} - 1/g_1 & T_{1,2} & T_{1,3} & \cdots & T_{1,N} \\ T_{2,1} & T_{2,2} - 1/g_2 & T_{2,3} & \cdots & T_{2,N} \\ T_{3,1} & T_{3,2} & T_{3,3} - 1/g_3 & \cdots & T_{3,N} \\ \vdots & \vdots & \vdots & \ddots & \vdots \\ T_{N,1} & T_{N,2} & T_{N,3} & \cdots & T_{N,N} - 1/g_N \end{pmatrix}, \tag{125}$$

from which the chemical potential in each site can be calculated as

$$\delta\mu_i = \sum_{j=1}^{N} \left[\mathbf{W^{-1}}\right]_{i,j} T_{j,0}\, \delta\mu_0. \tag{126}$$

Replacing these chemical potentials back in Eq. (123) the effective transmission can be calculated

$$\widetilde{T}_{R,L} = \underbrace{T_{R,L}}_{\text{coherent}} + \underbrace{\sum_{j=1}^{N}\sum_{i=1}^{N} T_{R,j}\left[\mathbf{W^{-1}}\right]_{j,i} T_{i,L}}_{\text{incoherent}}. \tag{127}$$

The right side contains two contributions: the first comes from electrons that propagate quantum *coherently* through the sample, the second contains the *incoherent* contributions due to electrons that suffer their first collision at site i and their last at site j.

Until now the procedure has been completely general, there is no assumption involving the dimensionality or geometry of the sample. The system of Fig.19 was adopted by DP only because it has a simple analytical solution for various situations ranging from tunneling to ballistic transport. We summarize the procedure for the linear response calculation. First, we calculated the complete Green's function in a tight binding model. With the Green's functions we then evaluate the transmittances between every pair of sites in the sample (i.e. nodes in the discrete equation) and write the transmittance matrix $\mathbf{W}$. Then, we solve for the current conservation equations that involves the inversion of $\mathbf{W}$.

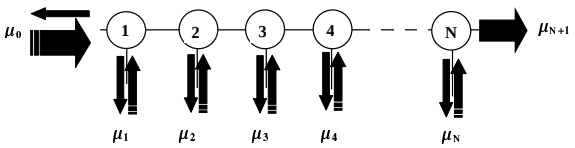

FIG. 19. Pictorial representation of the D'Amato-Pastawski model for the case of a linear chain.

What are the limitations of this model? A conceptual one is the momentum demolition produced by the localized scattering model. Therefore, we go directly from quantum ballistic description to a classical diffusive one. To describe the transition from quantum ballistic to classical ballistic, one should modify the model to have the scattering defined in momentum or energy basis.

The other aspect is merely computational. Since the resulting matrix $\mathbf{W}$ is no longer sparse, this inversion is done at the full computational cost. A physically appealing alternative to matrix inversion was proposed in DP. The idea was to expand the inverse matrix in series on the dephasing collisions, resulting in

$$\widetilde{T}_{R,L} = T_{R,L} + \sum_i T_{R,i} g_i T_{i,L} + \sum_i \sum_j T_{R,i} g_i T_{i,j} g_j T_{i,L} + \sum_i \sum_j \sum_l T_{R,i} g_i T_{i,j} g_j T_{j,l} g_l T_{l,L} + \ldots \tag{128}$$

The formal equivalence with the self-energy expansion of Matsubara and Toyosawa in terms of locators[45] or local Green's function justifies identifying g_i as a *locator* for the classical Markovian equation for the density[46] generated by the transition probabilities.

As an example of use of Eq. (128), one can readily apply it for the model of SectionVI A obtaining Eq.(117). This also constitutes the basis for a perturbative method of calculating the conductance with a substantially reduced computational cost. This strategy has been applied with considerable success to explain the stability of the Quantum Hall Effect[42] against scattering and dephasing.

Notice that Eq. (128) can also be rearranged as

$$\underbrace{\widetilde{T}_{R,L}}_{\text{total}} = \underbrace{T_{R,L}}_{=\text{coherent}} + \sum_{i=1}^{N} \underbrace{\widetilde{T}_{R,i}}_{+\text{ total}\times} \times \underbrace{g_i}_{1^{\text{st}}\text{ collision}\times} \times \underbrace{T_{i,L}}_{\text{coherent}} \tag{129}$$

The summation on the right hand side has the structure of the Dyson equation. It is a Bethe-Salpeter equation. This is graphically represented in Fig.20. We notice that according to the optical theorem $g_i = 2\pi\hbar\tau_\phi N_i$, while both transmittances entering the vertices in the figure are proportional to $1/\tau_\phi$ the whole product involved in the vertex is proportional to the dephasing rate. The arrows make explicit that transmittances are the product of a retarded (electron) and an advanced (hole) Green's function. To describe diffusive scattering by impurities one must replace the whole electron-hole pair by its ensemble average calculated in the ladder approximation, or eventually include their quantum corrections (see Ref.[46]).

Since the transmittance is essentially a two-particle Green's function, now it is a particular case of the Bethe-Salpeter equation which is solved in the "ladder" approximation which for the present model is exact (see appendix B in Ref.[46] for a detailed formalization of this picture with the Keldysh formalism). In summary, depending on the approximation used for the density propagator, the self-consistent solution contains the metallic transport, the weak-localization corrections and even the thermally activated hopping regime. It also can be viewed as a self-consistent Born approximation[47] for the electron-phonon interaction. One might also want to introduce other forms of interaction, such as those which

conserve momentum[48,49], but we will not extend on this point here.

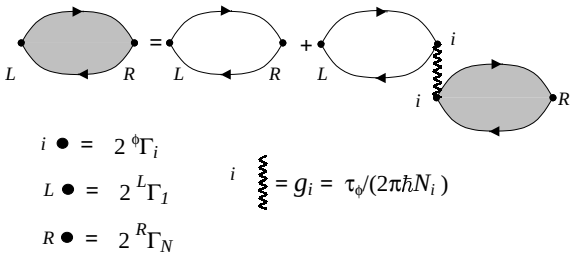

FIG. 20. Feynman Diagram for the Dyson Equation of the transmittance. It is equivalent to a particle-hole Green's function in the ladder approximation where the usual interaction rung connecting the two propagators is here represented by a dot.

Many of the results contained in the D'Amato-Pastawski paper for ordered and disordered systems were later extended in great detail in a series of papers by S. Datta and are described in his didactic book[35]. In the next section, we will illustrate how the previous ideas work by considering again our reference toy model for resonant tunneling.

D. Effects of decoherence in resonant tunneling

If we consider the "sample" to consist of a single state[50]. If we choose to absorb the energy shifts into the site energies $\widetilde{E}_0 = E_0 + \Delta_0(\varepsilon)$, the Green's function is trivial

$$G^R_{0,0}(\varepsilon) = \frac{1}{\varepsilon - \widetilde{E}_0 + \mathrm{i}(\ {}^L\Gamma_0 + \ {}^R\Gamma_0 + \ {}^\phi\Gamma_0)}. \tag{130}$$

By taking the Γ's independent on ε in the range of interest, we get the "broad-band" limit. We drop unneeded indices and arguments for the time being. From this Green's function all the transmission coefficients can be evaluated at the Fermi energy

$$\begin{aligned} T_{R,L} &= 4\ {}^R\Gamma\ \ |G_{0,0}|^2\ \ {}^L\Gamma, \\ T_{\phi,L} &= 4\ {}^\phi\Gamma\ |G_{0,0}|^2\ \ {}^L\Gamma, \\ T_{R,\phi} &= 4\ {}^R\Gamma\ \ |G_{0,0}|^2\ \ {}^\phi\Gamma. \end{aligned} \tag{131}$$

From the energy dependent transmittance we obtain the total transmittance

$$\begin{aligned} T_{R,L}(\varepsilon) = 4\ {}^R\Gamma & \frac{1}{\left(\varepsilon - \widetilde{E}_0\right)^2 + (\ {}^L\Gamma + \ {}^R\Gamma + \ {}^\phi\Gamma)^2} \\ & \times {}^L\Gamma \left\{1 - \frac{{}^\phi\Gamma}{{}^L\Gamma + {}^R\Gamma}\right\}. \end{aligned} \tag{132}$$

The first term in the curly bracket is the coherent contribution while the second is the incoherent one. We notice that the effect of the decoherence processes is to lower the value of the resonance from its original one in a factor

$$\frac{({}^L\Gamma + \ {}^R\Gamma)}{({}^L\Gamma + \ {}^R\Gamma + \ {}^\phi\Gamma)}. \tag{133}$$

In compensation, transmission at the resonance tails becomes increased.

It is interesting to note that if the resonant level lies between $\mu_o + eV$ and μ_o and provided that the voltage drop eV is greater than the resonance width $({}^L\Gamma + \ {}^R\Gamma + \ {}^\phi\Gamma)$, we take $T_{R,L}(\varepsilon, eV) \simeq T_{R,L}(\varepsilon)$ and we can easily compute the *non-linear response*. Notably, one gets that the total current does not change as compared with that in absence of decoherent processes, i.e.

$$\begin{aligned} \mathrm{I}\frac{h}{2e} &= \int_{\mu_o}^{\mu_o + eV} \widetilde{T}_{R,L}(\varepsilon) d\varepsilon \\ &= \int_{\mu_o}^{\mu_o + eV} T^o_{R,L}(\varepsilon) d\varepsilon \\ &= 4\pi\ {}^R\Gamma \frac{1}{({}^L\Gamma + \ {}^R\Gamma)}\ {}^L\Gamma. \end{aligned} \tag{134}$$

Thus, in this extreme quantum regime, the decoherence processes do not affect the overall transport.

In spite of the complexity of the general problem of decoherence in mesoscopic systems we extract an important lesson from the case of resonant tunneling with decoherence solved above within the DP model. The inclusion of external degrees of freedom has three effects

1) It broadens the resonance relaxing energy conservation.

2) The integrated intensity of the elastic (coherent) peak is decreased.

3) The inelastic contribution came out to compensate this loss and maintains the value of the total transmittance integrated over energy.

4) Taking this system as representative of those whose spectra are strongly quantized, i.e. with well defined, isolated resonances, one may state that these systems are quite stable against decoherence.

VII. THE SOLUTION OF TIME DEPENDENCE

First we remember that the Green's function gives the possibility to write non trivial initial values in the space-time coordinate $X_j = (\mathbf{r}_j, t_j)$ described by $\varphi_{\mathrm{source}}(X_j)$. Therefore, any wave function injected at space time $X_j = (\mathbf{r}_j, t_j)$ by an arbitrary source is propagated by the retarded Green's function

$$\varphi(X_2) = \mathrm{i}\hbar \int G^R(X_2; X_j)\varphi_{\mathrm{source}}(X_j)\mathrm{d}X_j \tag{135}$$

Here, instead of using a discrete spatial index, we adopted the notation $G^R_{\mathbf{r}_2,\mathbf{r}_j}(t_2;t_j) \rightarrow G^R(X_2;X_j)$ and

$\sum_{\mathbf{r}_j}\int \mathrm{d}t_j \to \int \mathrm{d}X_j$. To inject particles with some definition in momentum and/or energy we need to introduce precise correlation between space and time variables. We resort to the complementary equation

$$\varphi^*(X_1) = -\mathrm{i}\hbar \int \varphi^*_{\mathrm{source}}(X_k) G^A(X_k;X_1)\mathrm{dX_k}, \quad (136)$$

which we can use to find how the density matrix of particles depends on both correlated initial conditions

$$[\varphi^*(X_1)\varphi(X_2)] = \hbar^2 \int\int G^R(X_2,X_j) \times [\varphi_{\mathrm{source}}(X_j)\varphi^*_{\mathrm{source}}(X_k)]\, G^A(X_k,X_1)\mathrm{dX_j}\mathrm{dX_k} \quad (137)$$

The usual density function is defined by taking $X_1 = X_2$ i.e. $\rho(X_1) = \varphi^*(X_1)\varphi(X_1)$. This is nothing else but the Schrödinger equation written in a general form that allows arbitrary boundary conditions $[\varphi_{\mathrm{source}}(X_j)\varphi^*_{\mathrm{source}}(X_k)]$. One is used to the initial conditions at space-time coordinate X_i of the form $\rho_{\mathrm{source}}(X_i) = [\varphi_{\mathrm{source}}(X_i)\varphi^*_{\mathrm{source}}(X_i)]$ which allows precision in the specification of position and time at the price of absolute uncertainty in momentum and energy. The formalism allows one to program an uncertainty tradeoff to approach better to a semiclassical initial condition with energy and momentum known up to some precision.

The basic idea to get the physics of time dependent phenomena from Eqs. (137) or from its generalization in Quantum Fields Theory[32,33] is to recognize that in any Green's function $G(t_j;t_k)$, a macroscopically observable time is $t = \frac{1}{2}[t_j + t_k]$ whose Fourier transform is an observable frequency ω. Meanwhile, system's microscopic energies, ε, are Fourier transforms of internal time differences $t_j - t_k$. By operating carefully with this concept in Eq. (137), the dynamical transmittances $T(\mathbf{r}_f,\mathbf{r}_i;\varepsilon,\omega) \equiv T_{f,i}(\varepsilon,\omega)$ with $\mathbf{r}_i$ a position in channel i and $\mathbf{r}_f$ a position in channel f are obtained. The manipulation of the time integrals is quite subtle and we refer to Ref.[50] for details. The basic result is

$$T_{f,i}(\varepsilon,\omega) = 2\Gamma_f G^R_{f,i}(\varepsilon + \frac{1}{2}\hbar\omega) 2\Gamma_i G^A_{i,f}(\varepsilon - \frac{1}{2}\hbar\omega), \quad (138)$$

and is consistent with the steady-state Fisher-Lee equation. From this new formula we can evaluate the probability that the wave packet of mean energy ε propagates from i to f in a time t as

$$T_{f,i}(\varepsilon,t) = \int T_{f,i}(\varepsilon,\omega)\exp[-\mathrm{i}\omega\mathrm{t}]\frac{\mathrm{d}\omega}{2\pi}. \quad (139)$$

This time dependent transmittance was incorporated in a generalization of the Landauer formula for time dependent phenomena.

Since the spectrum is continuous we can keep the lowest order in the frequency expansion and obtain

$$T_{f,i}(\varepsilon,\omega) \simeq \frac{T_{f,i}(\varepsilon)}{1 - \mathrm{i}\omega\tau_{\mathrm{P}}}. \quad (140)$$

Clearly, such approximation would give an exponential for the propagation dynamics which does not describe the very short time regime. According to Eq.(4.5) in Ref.[50], the typical propagation time τ_P between points r_i and r_f results

$$\tau_P = \frac{\mathrm{i}\hbar}{2}\left[G^R_{f,i}(\varepsilon)\frac{\partial}{\partial\varepsilon}G^R_{f,i}(\varepsilon)^{-1} + G^A_{i,f}(\varepsilon)\frac{\partial}{\partial\varepsilon}G^A_{i,f}(\varepsilon)^{-1}\right] \quad (141)$$
$$= -\frac{\mathrm{i}\hbar}{2}\frac{\partial}{\partial\varepsilon}\ln\frac{G^R_{f,i}(\varepsilon)}{G^A_{i,f}(\varepsilon)}$$

This was evaluated in various simple systems in Ref.[50]. There, for *b*allistic metals with velocity v_ε one gets $\tau_P = |\mathbf{r}_f - \mathbf{r}_i|/v_\varepsilon$. For *d*iffusive metals where impurity collision at a rate $1/\tau_o$ determines the diffusion constant $D_\varepsilon = v_\varepsilon^2\tau_o/2$ it results $\tau_P = |\mathbf{r}_f - \mathbf{r}_i|^2/(2D_\varepsilon)$.

As a striking example, we mention the "simple" case of *tunneling through a barrier*[51] of length L and height U exceeding the kinetic energy ε of the particle. One gets

$$\tau_P = \frac{L}{\sqrt{\frac{2}{m}(U-\varepsilon)}}, \quad (142)$$

which, within our non-relativistic description, can be extremely short (even superluminal[52]!) provided that the barrier is high enough.

In a double barrier system, in the regime of *resonant tunneling,* the above contribution becomes negligible and the propagation time is then fully determined by the lifetime inside the well. In fact, by using the functions of the previous Section, one gets a delay of

$$\tau_P = \frac{\hbar}{2(\,{}^L\Gamma + {}^R\Gamma)} \quad (143)$$

which readily limits the admittance associated to the device to $\mathsf{G}(\omega) = \mathsf{G}(0)/(1 - \mathrm{i}\omega\tau_P)$. This is in fair agreement with the experimental results[53]. Tunneling times can also be calculated in more complex situations such as disordered[54]systems and situations with coherent capacitive effects and phonon interactions[55] and decoherent[50]processes..

VIII. FINAL REMARKS.

We hope these lectures have been able to convey, at least partially, the essence of our message: In our attempt to understand the quantum world it is possible, and convenient, to make very simple models of nature. Those models, though not necessarily complete, can show us many effects that surprise our classical intuition and which would have been obscured by other more "complete" descriptions. Every one of these surprises can give a new twist in the experimental research, which is indeed

the ultimate truth, and eventually become the source of an innovative application.

In our toolbox to extract information from the proposed models the most important elements have been the decimation method and the Green's functions technique. Both are intimately connected with the renormalization group concept. As such they are fundamental in generating the models themselves, as they help us to identify the relevant variables. Simultaneously, our understanding of the quantum world has benefited from fresh approaches to long standing problems as that of the tunneling time. In the process of computing transport properties we have also learnt the deepest principles of statistical mechanics as to what is the origin of macroscopic irreversibility and established the conditions for the validity of the ergodic hypothesis. The fundamentals of decoherent processes in transport and their consequences are currently of intense interest. The lines of thought we have sketched here, have turned out to be very productive in this direction, and we hope they will continue being fruitful through the action of our students.

---

[1] L. Esaki, Rev. Mod. Phys. **46**, 237 (1974).

[2] V. J. Goldman, D. C. Tsui and J. E. Cunningham, Phys. Rev. Lett. **36**, 7635 (1987).

[3] B. L. Altshuler, P. A. Lee and R. A. Webb, eds. *Mesoscopic Phenomena in Solids* (North-Holland, Amsterdam, 1991); C. Weisbuch and B. Vinter, *Quantum Semiconductor Structures, Fundamentals and Applications*, (Academic Press, San Diego, 1991); E. Akkermans, G. Montambaux, J.-L. Pichard and J. Zinn-Justin, eds. *Mesoscopic Quantum Physics,* (Elsevier, Amsterdam 1995).

[4] M. A. Reed and J. M. Tour, Sci. Am. **282** (6), 68 (2000).

[5] K. V. Mikkelsen and M. A. Ratner, Chem. Rev. **8**7, 113 (1987).

[6] A. J. Heeger, S. Kivelson, J. R. Schrieffer and W. -P. Su, Rev. Mod. Phys. **60**, 781 (1988).

[7] H. Taube, Inorg. Chem, **20**, 3124 (1981); C. Creutz, Progr. Inorg. Chem. **30**, 1 (1983).

[8] D. N. Beratan and J. J. Hopfield, J. Am. Chem. Soc. **106**, 1584 (1984); D. N. Beratan, J. N. Beatts and J.N. Onuchic, Science **252**, 1285 (1991).

[9] R. Landauer, IBM J. Res. Develop. **1**, 223 (1957); R. Landauer, Philos. Mag. **21**, 863 (1970).

[10] M. Kastner, Physics Today **46**, 25 (1993).

[11] M. H. Devoret, D. Esteve and C. Urbina, Nature **360** 547 (1992).

[12] L. P Kouwenhoven, C. M. Marcus, P. L. McEwen, S. Tarucha, R. M.Westervelt and N. Wingreen, in *Procc. of the Advanced Study Institute on Mesoscopic Electron Transport*, L. L. Sohn, L. P. Kouwenhoven and G. Schön, edts. (Kluwer 1997)

[13] L. I. Schiff, *Quantum Mechanics*, McGraw-Hill (New York, 1949).

[14] M. Büttiker, Phys. Rev. Lett. **57**, 1761 (1986).

[15] P. Levstein, H. M. Pastawski and J. L. D 'Amato, *J. Phys.: Condens. Matter* **2**, 1781 (1990).

[16] P. O. Löwdin, J. Chem. Phys. **19**, 1396 (1951).

[17] These projection techniques were discussed in the context of a real space Renormalization Group Decimation in: C.E.T. Gonçalves da Silva and B. Koiller, *Solid St. Comm.* **40**, 215 (1981) and J. B. Sokoloff and J. V. José, *Phys. Rev. Lett.* **49**, 334 (1982); E. Domany, S. Alexander, D. Bensimon and L. Kadanoff, Phys. Rev. B, **28,** 3110 (1983).

[18] R. D. Mattuck, *A guide to Feynman diagrams in the many-body problem* (2nd ed.) McGraw-Hill (1976).

[19] H. M. Pastawski, J. F. Weisz and S. Albornoz, Phys. Rev B. **28**, 6896 (1983); H. M. Pastawski, C. Slutzky and J. F. Weisz, *ibid.* **32**, 3642 (1985).

[20] V. Mujica, M. Kemp and M. A. Ratner, J. Chem. Phys. **101**, 6856 (1994); M. D. Coutinho Neto and A. A. daGama, Chem. Phys. **203**, 43 (1996); J. N. Onuchic, P. C. P. de Andrade and D. N. Beratan, J. Chem. Phys. **95**, 1131 (1991).

[21] U. Fano, Phys. Rev. **124** 1866 (1961).

[22] J. F. Weisz and H. M. Pastawski, Phys. Lett. A **105**, 421 (1984).

[23] B. Kramer and A. MacKinnon, Rep. Prog. Phys. **56**, 1469 (1993).

[24] H. M.Pastawski and C. Wiecko, Phys. Rev. A. **36**, 5854 (1987).

[25] D. C. Mattis and R. Raghavan, Phys. Lett. A **75**, 3313 (1980).

[26] V. N. Prigodin, B. L. Altshuler, K. B. Efetov and S. Iida, Phys. Rev. Lett., **72**, 546 (1994); H. M. Pastawski, P. R. Levstein and G. Usaj, Phys. Rev. Lett. **75**, 4310 (1995); Pastawski, H. M., G. Usaj and P. R. Levstein, Chem. Phys. Lett. **261**, 329 (1996).

[27] F. M. Cucchietti, H. M. Pastawski, G. Usaj and E. Medina, Anales AFA **10**, 224 (1998).

[28] J. L. D 'Amato, H. M. Pastawski and J. F. Weisz, Phys. Rev. B **39**, 3554 (1989).

[29] Y.-Ch. Chang, L. L. Chang and L. Esaki, Appl. Phys. Lett. **47**, 1324 (1985).

[30] F. Sols, M. Macucci, U. Ravaioli and K. Hess, Appl. Phys. Lett. **54**, 350 (1989).

[31] W. Wegscheider, L. N. Pfeiffer, M. M. Dignam, A. Pinczuk, K. W. West, S. L. McCall and R, Hull, Phys. Rev. Lett. **71**, 4071 (1993).

[32] L. V. Keldysh, Zh. Eksp. Teor. Fiz. **91**, 1815 (1986) [Sov. Phys. JETP **64** 1075 (1986)]; L. P. Kadanoff and G. Baym, *Quantum Statistical Mechanics* (Benjamin, New York, 1962).

[33] P. Danielewicz, Ann. Phys. (N. Y.) **152**, 239 (1984).

[34] D. S. Fisher and P. A. Lee, Phys. Rev. B **23**, 6951 (1981); F. Sols, Ann. Phys. (N.Y.) **214**, 386 (1992).

[35] S. Datta, J. Phys. Cond. Matter **2**, 8023 (1990), *Electronic Transport in Mesoscopic Systems*, Cambridge U. P. (Cambridge, 1995) and references therein.

[36] J. L. D'Amato and H. M. Pastawski, Phys. Rev. B **41**, 7411 (1990).

[37] S. Washburn and R. A. Webb, Adv. Phys. **35**, 375 (1986).

[38] B. L. Altshuler, A. G. Aronov, and B. Z. Spivak, Pis'ma Zh. Eksp. Teor. Fiz. 33, 101 (1981) [JETP Lett. **33**, 94 (1981)]

[39] E. Medina and H. M. Pastawski, Phys. Rev. B **61**, 5850 (2000), and references therein.
[40] D. A. Wharam et al, J. Phys. C **21**, L209 (1988); B. J. Van Wees et al, Phys. Rev. Lett. **60**, 848 (1988).
[41] M. Büttiker, Phys. Rev. B, **38**, 9775 (1988).
[42] F. Gagel and K. Maschke, Phys. Rev. B **54**, 13889 (1996).
[43] S. Washburn and R. A. Webb, Rep. Prog. Phys. **55**, 1311 (1993).
[44] M. Büttiker. IBM J. Res. Develop. **32**, 63 (1988).
[45] T. Matusbara and Y. Toyosawa, Prog. Theor. Phys. **26**, 739 (1961); see also: J. M. Ziman, *Models of Disorder*, Cambridge Univ. Press (Oxford 1979).
[46] H. M. Pastawski, Phys. Rev. B **44**, 6329 (1991).
[47] S. Hershfield, Phys. Rev. B **43**, 11586 (1991).
[48] I. Knittel, F. Gagel and M. Schreiber, Phys. Rev. B, **60**, 916 (1999).
[49] P. W. Brouwer and C. W. J. Beenakker, Phys. Rev. B **55**, 4695 (1997).
[50] H. M. Pastawski, Phys. Rev. B **46**, 4053 (1992).
[51] M. Büttiker and R. Landauer, Phys. Rev. Lett. **49**, 1739 (1982); R. Landauer, Nature **341**, 567 (1989); R. Landauer and Th. Martin, Rev. Mod. Phys. **66**, 217 (1994).
[52] D. Mugnai, A. Ranfagni, and R. Ruggeri, Phys. Rev. Lett. **84**, 4830 (2000).
[53] E. R. Brown, T. C. L. G. Sollner, C. D. Parker, W. D. Goodhue, and C. L. Chen, Appl. Phys. Lett. **55**, 1777 (1989).
[54] C. J. Bolton-Heaton, C. J. Lambert, V. I. Falco, V. Prigodin and A. J. Epstein, Phys. Rev. B **60**, 10569 (1999).
[55] H. Haug and A.-P. Jauho. *Quantum Kinetis in Transport and Optics of Semiconductors*. Springer-Verlag (Heidelberg, 1998); A. P. Jauho, N. S. Wingreen and Y. Meir, Phys. Rev. B **50**, 5528 (1994).